2015

Generation of 2-Adamantylidenecarbene from a Phenanthrene-Based Precursor

Christine E. Wamsley
Colby College

Generation of 2-Adamantylidenecarbene
from a Phenanthrene-based Precursor

Christine E. Wamsley

Approved:

Dasan M. Thamattoor, Ph.D., Advisor
Professor of Chemistry

Date

Reuben H. Hudson
Chemistry Post Doctorate Fellow

Date

“Success is no accident. It is hard work, perseverance, learning, studying, sacrifice and most of all, love of what you are doing or learning to do.”
- Pelé

“Fail to prepare, prepare to fail.”
- Roy Keane

“Impossible is just a big word thrown around by small men who find it easier to live in the world they’ve been given than to explore the power they have to change it. Impossible is not a fact. It’s an opinion. Impossible is not a declaration. It’s a dare. Impossible is potential. Impossible is temporary. Impossible is nothing.”
- Muhammad Ali

Acknowledgements

First and foremost, I would like to thank my parents for their undying love and support. Even when I did not think I could complete all that I set out to do at Colby, your comfort and encouragement gave me the strength to keep going. Thank you for showing me what hard work looks like.

Additionally, I would like to acknowledge the Chemistry department and all of the professors and teaching assistants I have had over the past four years. The faculty has helped me improve not only as a student, but as a person as well. I am thankful for the insight and knowledge they have shared not only with me, but with all of the students in their classes.

Last and certainly not least, I would like to thank my advisor, Das. Having you as a sophomore for Organic Chemistry inspired me to become a Chemistry major, and I have never looked back. Your passion and enthusiasm not only made Chemistry enjoyable, but your dedication to making sure every student has the chance to succeed is something I will never forget. Thank you for having the confidence in me to pursue this thesis, and I am forever grateful for all of the patience and support that you have shown me along the way.

Table of Contents

Abstract

This thesis examines the generation of 2-adamantylidenecarbene from a phenanthrene-based precursor. A three-step synthetic procedure was used to generate the 2-adamantylidenecarbene precursor, which subsequently underwent photolysis to produce 2-adamantylidenecarbene. This product was trapped with cyclohexene. No evidence of a ring expansion to 4-homoadamantyne was observed. It was also noted that the target precursor underwent rearrangement during photolysis, leading to the formation of an isomer containing a seven-membered ring. This isomer did not photolyze. Additionally, computational studies were performed using Gaussian 09. Geometries were initially optimized and then, the single point energies of the singlet and triplet carbene states were calculated. It was found that the singlet 2-adamantylidenecarbene is energetically more stable. Finally, the transition barrier between the singlet 2-adamantylidenecarbene and 4-homoadamantyne was calculated to be 24.8 kcal/mol.

Introduction
1.1 Carbenes

The carbene is an intermediate consisting of a neutral, divalent carbon covalently linked to two groups and two valence electrons. The species is electron deficient. The parent carbene, methylene, is simply a carbon atom with two hydrogen atoms covalently attached.[1]

Although the term carbene was first coined by Doering, Winstein, and Woodward in 1951, several attempts were made earlier to generate methylene.[1] The first efforts to prepare this compound began in 1836, when Dumas and Regnault tried to dehydrate methanol by phosphorous pentoxide or concentrated sulfuric acid, all while avoiding oxidation of the carbon atom.[2,3] Further studies attempted to eliminate hydrogen chloride from chloromethane via pyrolysis and to reduce methylene iodide with copper powder.[4,5] However, both groups were unsuccessful; the latter experiment only generated ethylene. A second period of carbene research began as a result of the discovery of isonitriles/isocyanides and fulminic acid derivatives. During this time, Nef proposed the "general methylene theory," arguing that most substitution reactions occur via α-elimination and addition. However, his claims about carbene chemistry were widely unaccepted by other chemists of the time.[6] Finally, a breakthrough occurred in 1912 when Staudinger and his associates began focusing on the potential in the breaking down of diazo compounds and ketenes. They concluded that carbenes are a transient species.[7-10]

Since then, carbene research has rapidly expanded and much has been discovered about the nature of this species and its potential synthetic uses. As previously mentioned, the neutral carbon atom in carbene only possesses two of the four possible bonds that it can form. Consequently, the carbene is distinguished by the positioning of the two remaining electrons. These two unpaired electrons can be paired or unpaired. If the two electrons occupy the same

hybridized sp^2 orbital and have antiparallel spins, they are in the singlet state. If they are split between the sp^2 and p orbitals of the carbon and exhibit parallel spins, the electrons are in the triplet state, as they have a net electronic angular momentum of 1 (Figure 1).

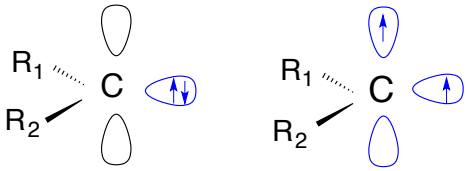

Figure 1. The singlet and triple states of carbene. In the singlet configuration, two paired electrons occupy the same sp^2- hybridized orbital. In the triple configuration, one electron occupies each orbital and they exhibit parallel spin.

According to Hund's rule, the two electrons will not occupy the same orbital until all orbitals in a given subshell are filled. This minimizes the repulsion of like charges and accordingly, produces the most energetically stable configuration. Therefore, the triplet state for most carbenes is considered the lower energy state. However, the singlet state could be lower in energy if the adjacent groups attached to the carbon atom are strongly electron-donating to the carbon's empty p-orbital. Therefore, the spin state of carbenes are largely determined by the nature of the functional groups attached to the divalent carbon atom. Neighboring groups that are unable to donate electrons to the carbene generally result in a triplet state, and groups that donate electrons stabilize the singlet form by supplying electrons to the empty p-orbital.

Based on the reactive nature of these valence electrons, carbenes normally have very short lifetimes. Therefore, it has proven difficult to characterize carbenes until recently. In 1991, Arduengo generated the first stable carbene, 1,2-diadamantylimidazol-2-ylidene 1 (Figure 2).[11] Since then, extensive research has been done in attempts to stabilize and isolate carbenes.

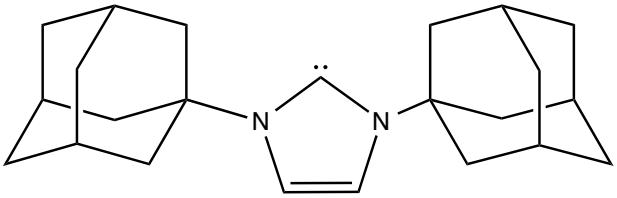

Figure 2. The first stable carbene to be synthesized was 1,3-diadamantylimidazol-2-ylidene.

1.2 Carbene Reactivity

Carbene reactivity is influenced by the spin states of the valences electrons and the functional groups attached to the carbon atom. Singlet carbenes can exert nucleophilic or electrophilic activity; the paired electrons are well aligned for bond formation; however, the empty p-orbital is also open to attack by a nucleophile.[1] The three types of reactions that singlet carbenes can undergo are shown below. σ-Bond interactions occur when the carbene carbon is inserted between two atoms that were previously joined by a σ-bond; the two substituent functional groups on the carbene also accompany the carbon atom. Intramolecular rearrangements of carbenes involve the movement of an adjacent group to the divalent carbon (Figure 3). Finally, cycloadditions of singlet carbenes to π-bonds is fairly predictable and results in the formation of a three-membered ring. The reaction is stereospecific through a single step, concerted process (Figure 4).[12,13]

(I)

(II)

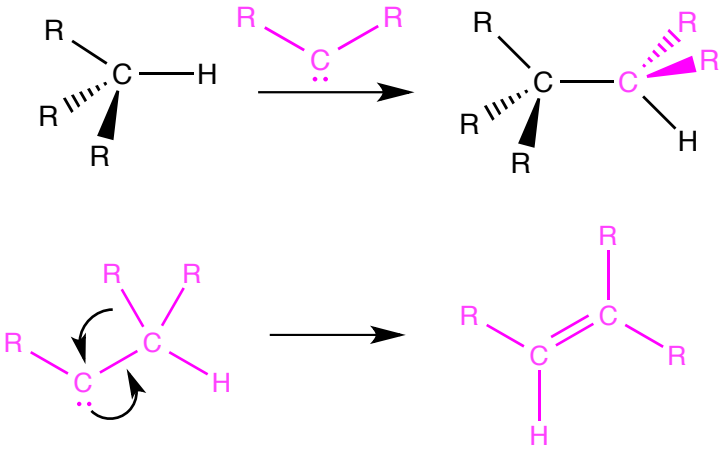

Figure 3. (I) Singlet carbenes are known to react via (I) σ-bond insertion and (II) intramolecular rearrangements.

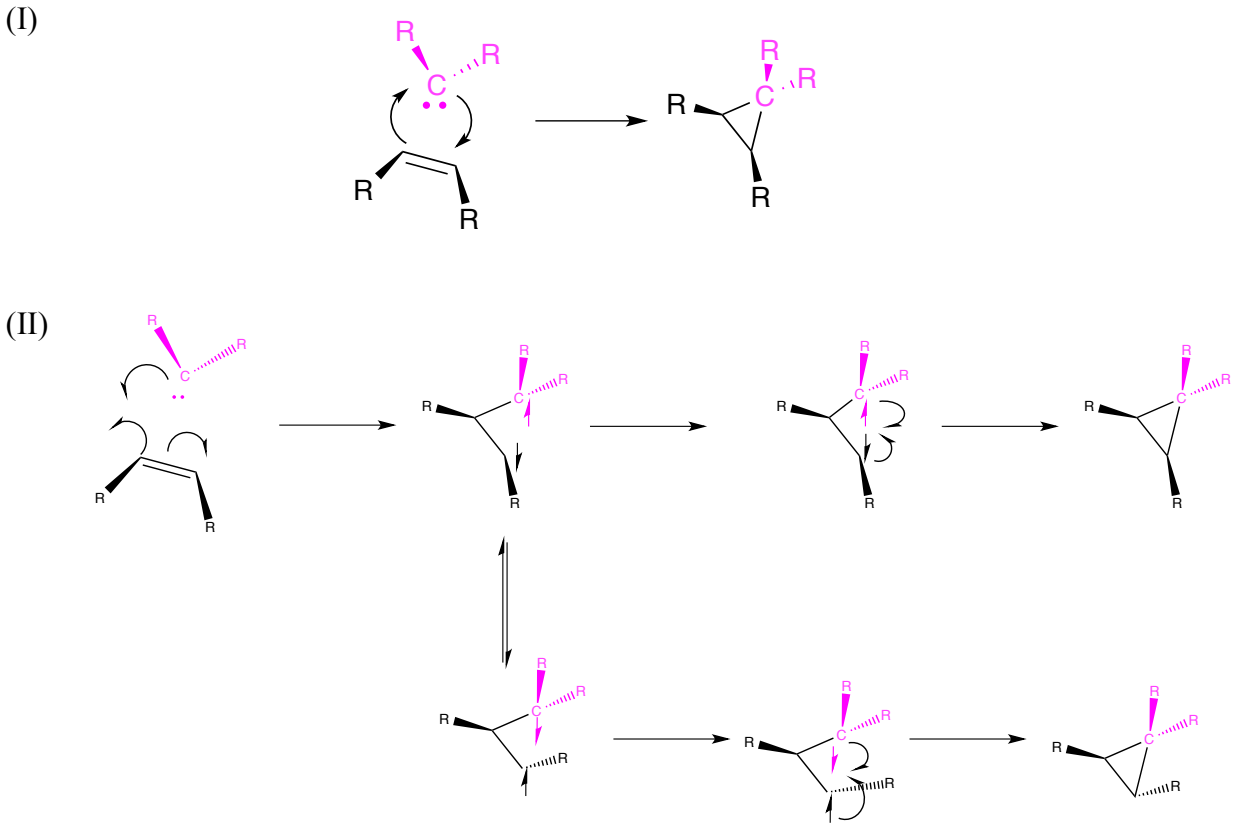

Figure 4. (I) Singlet carbene addition to π-bonds preserves the stereochemistry of the alkene, while (II) triple carbene addition occurs in multiple steps, and thus, stereochemistry may be lost.

Triplet carbenes, on the other hand, exhibit more electrophilic activity and behave similarly to diradicals. This can be seen in their cycloaddition reactions with π-bonds. Ring formation occurs in a multi-step process, as the parallel spins cannot immediately come together to form a bond. During the time it takes one electron to undergo a spin-flip, rotation about the bond may occur. Therefore, the stereochemistry in the final products may be scrambled upon bond formation (Figure 4).[12,13]

1.3 Forming Carbenes

There are several general methods for producing carbenes. Often, they require the starting material to have a good leaving group, so that upon departure of this group, a carbene will be produced. This reaction can be accelerated with heat, light, or a catalyst.

The first way of producing a carbene is via a haloform and strong base.[14] Haloforms, such as bromoform, can be reacted with a strong base in order to extract a proton and generate an anionic intermediate. As halogens are stable leaving groups, one of them may be removed, a process called α-elimination, resulting in the formation of a carbene (Figure 5).

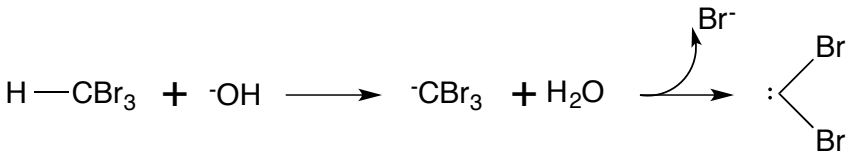

Figure 5. The reaction of bromoform with a strong base results in the departure of a bromide ion and the formation of a dibromo-carbene.

Perhaps the most common method of producing carbenes is via diazo compounds. Photolytic or pyrolytic decomposition of these molecules results in the liberation of nitrogen gas and a carbene product (Figure 6).[15] Although diazo compounds are useful intermediates in organic synthesis of carbenes, these nitrogenous precursors are quite toxic and can exhibit unpredictable explosive, mutagenic, and carcinogenic behavior.

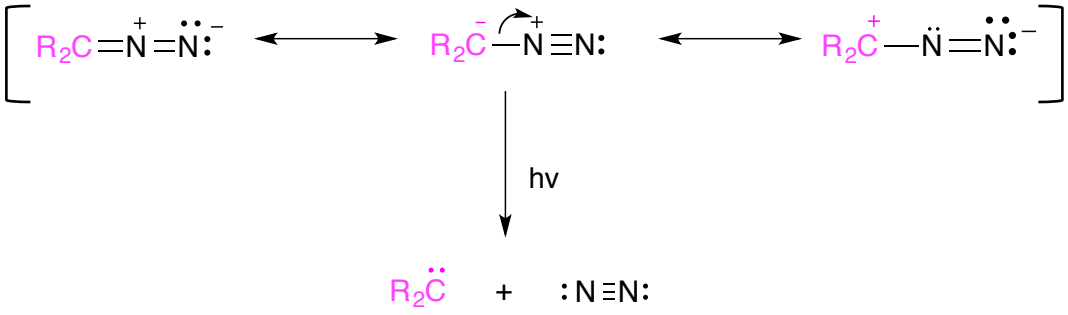

Figure 6. Carbenes can also be formed from diazoprecursors. Photolytic decomposition results in the formation of nitrogen gas and a carbene.

In order to avoid these hazards, another method of generating carbenes via phenanthrene-based precursors has been developed. Carbene generation is driven by the rearomatization of the precursor backbone, allowing the departure of a carbene product. This process can be accelerated via photolysis with UV light. This method has resulted in the successful production of methylene and other carbenes (Figure 7).[17]

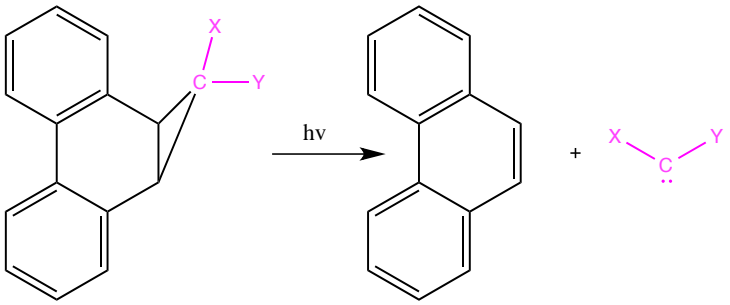

Figure 7. Carbenes can be formed using phenanthrene-based precursors. The reaction is driven by the formation of stable aromatic molecules, which can be accelerated via photolysis.

1.4 Generating 2-adamantylidenecarbene, a caged vinylidenecarbene

This study focuses on the generation of a caged vinylidenecarbene, 2-adamantylidenecarbene. This work is an extension of previous research that has been conducted in the laboratory. While studies have shown that photolytic cleavage of the phenanthrene-based precursor produces a carbene, Kathryn Moore and Jesus Vidaurri investigated whether the carbon must have two covalently attached functional groups, along with the two bonds that are cleaved to generate a carbene. They found that a carbene carbon connected to a double bond can also undergo photolytic cleavage, generating a vinylidenecarbene. (Figure 8).[19]

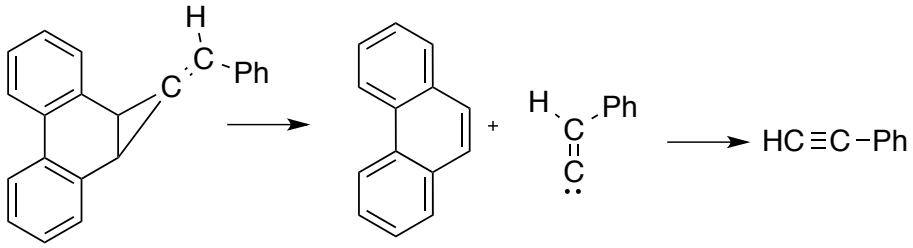

Figure 8. 1-Benzylidene-1a,9b-dihydro-1H-cyclopropa[l]phenanthrene was used as a phenanthrene-based precursor to generate benzylidenecarbene and phenanthrene via photolytic cleavage. The carbene subsequently rearranged to phenylacetylene.

Following the successful generation of a vinylidenecarbene, Daniel Mauer examined whether cyclic vinylidenecarbenes could be accessed through photochemical methods, in which the two groups coming off the β-carbon of the resulting carbene are tied up in a ring structure. He found that, indeed, photolytic cleavage did occur. The resulting carbene contained two covalently-attached functional groups that were tied together in a five-membered ring structure. This carbene subsequently underwent a ring expansion to generate a six-membered cyclic alkyne. Finally, this product was trapped by an olefin, as shown in Figure 9.[20]

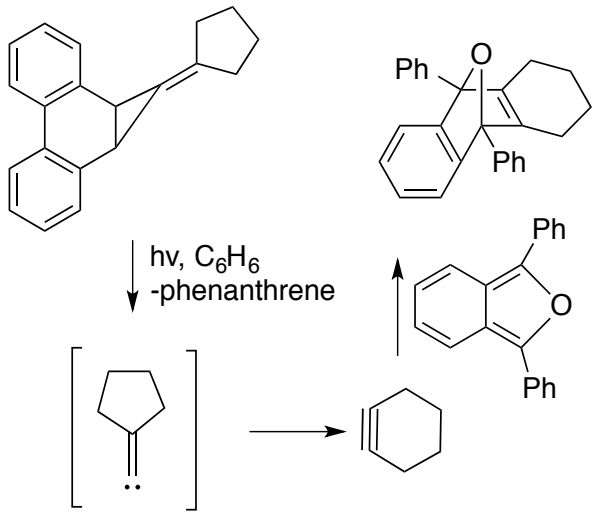

Figure 9. Cyclopentylidenecarbene can be generated by photolytic cleavage of a phenanthrene-based precursor. The product shown above rearranged to a cyclic alkyne via ring expansion and was subsequently trapped by an olefin.

Building upon these results, this study examined whether caged vinylidenecarbenes can be accessed photochemically. In order to determine this, the following target precursor (**7**) was syntheseized (Figure 10**)**. Successful photolytic cleavage of this phenanthrene-based precursor should result in the formation of phenanthrene and 2-adamantylidenecarbene (**12**). In this study, we also investigated whether 2-adamantylidenecarbene could be trapped and if it also rearranged to 4-homoadamantyne (**13**), a caged cyclic alkyne (Figure 10).

(I)

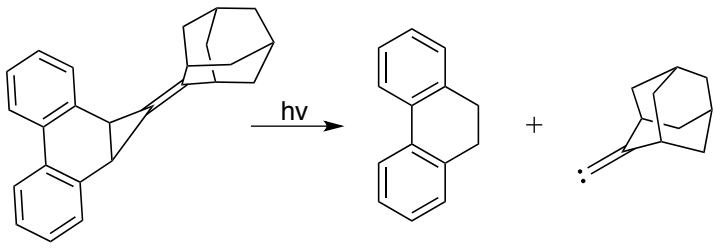

7 **12**

(II)

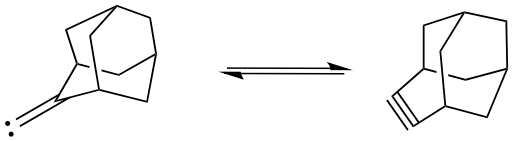

13

Figure 10. (I) Through successful photolytic cleavage of the target precursor, the phenanthrene backbone should rearomatize to phenanthrene, expelling 2-adamantylidenecarbene. (II) The ring expansion to form 4-homoadamantyne was also investigated in this study.

Previous studies have shown that 2-adamantylidenecarbene can, in fact, be made, although generation via photochemical processes has not yet been explored. In 1978, Sasaki *et al*. published their results that the combination of ω-bromomethyleneadamantane and potassium *t* –butoxide with a crown ether catalyst produced 2-adamantylidenecarbene.[21] Six years later, the group published another paper reporting that they trapped the 2-adamantylidenecarbene product with cyclohexene (Figure 11).[22] Sasaki and his research group, however, concluded that 2-adamantylidenecarbene did not subsequently rearrange to 4-homoadamantyne as the adamantyne was too strained to expand or contract; they claimed that the resulting product only existed in its carbene form, which was subsequently trapped with cyclohexene.[21]

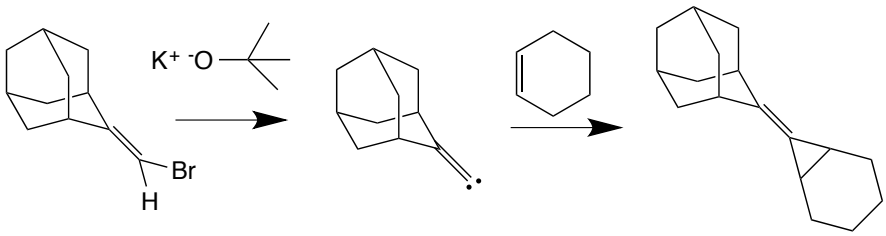

Figure 11. Sasaki *et. al* generated 2-adamantylidenecarbene in 1978 using *ω*-bromomethyleneadamantane and potassium *t* –butoxide. Following this, they trapped the carbene product with cyclohexene.

In 1991, Komatsu *et. al*, published somewhat contradicting results, in terms of the generation of 4-homoadamantyne. In their experiment, BuLi was first added to 4,5-dibromo-4-homoadamantene. Following this, LiBr was eliminated, producing the 4-homoadamantyne that Sasaki *et al*. claimed could not be generated from the carbene. In order to substantiate the formation of the caged alkyne, the compound was reacted with $Pt(PPh_3)$, resulting in its trapping (Figure 12). Although Komatsu and his group synthestized 4-homoadamantyne by a different method than Sasaki *et. al*. attempted, they reported no carbene products at the end of the reaction. There was no mention of the ring contraction that Sasaki *et. al*. claimed was inevitable.[23]

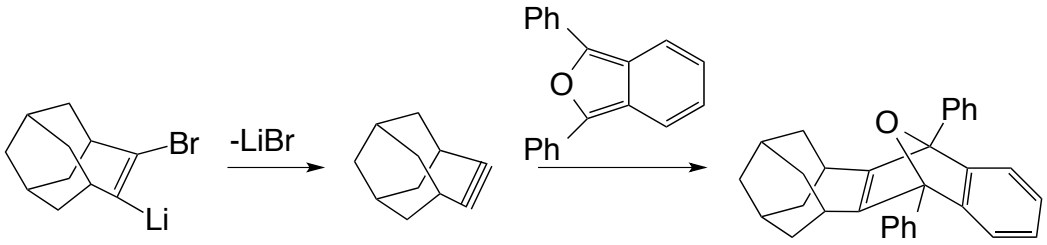

Figure 12. In 1991, Komatsu *et al.* claimed to have generated 4-homoadamantyne and subsequently trapped this caged alkyne by an olefin.

The objectives of this study are, therefore, twofold. After generating the 2-adamantylidenecarbene precursor (**7**) through a three-step synthesis, the photolytic cleavage of this target precursor to produce 2-adamantylidenecarbene (**12**) was investigated (Figure 10). Additionally, the possibility of ring expansion to a caged alkyne was explored.

Results and Discussion

2.1 Synthetic Aspects

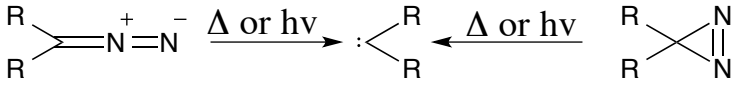

1 **3** **2**

Scheme 1. Generating Carbenes from Nitrogenous Sources

The traditional method of generating carbenes, as shown in Scheme 1, involves the photochemical and/or thermal decomposition of nitrogenous precursors. While these precursors serve their purpose well, they are often hazardous and particularly explosive to handle. Additionally, the desired nitrogenous precursor may not be available. Therefore, generating carbenes through an alternative route can be a useful tool to chemists wishing to study this intermediate.

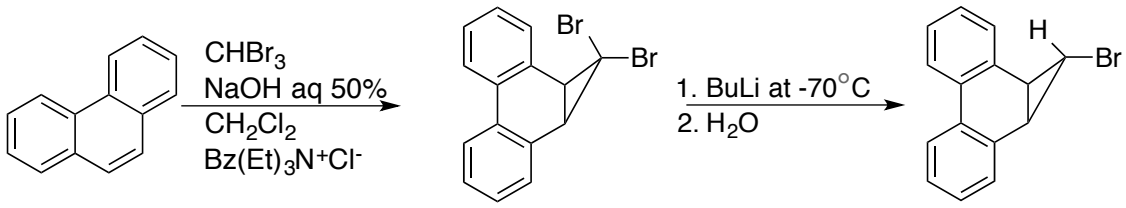

4 **5** **6**

Scheme 2. Synthesis of 1-Bromo-1a-dihydrocyclopropa[*l*]phenanthrene (6) from Phenanthrene (4)

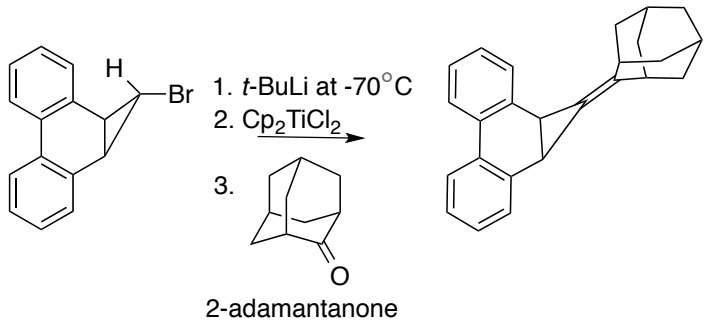

7

Scheme 3. Synthesis of the Target Precursor (7) via the Petasis Reaction

For this study, the approach to synthesizing the 2-adamantylidenecarbene precursor consisted of a three-step process starting from commercially available phenanthrene (**4**), as shown in schemes 2 and 3. In the first step, a phase-transfer catalyst, benzylthriethylammonium chloride, and aqueous sodium hydroxide were used to form 'CBr_2' with phenanthrene in a heteregenous medium. Along with producing substantial yields, this simple synthesis can be carried out under ambient conditions in an Erlenmeyer flask, followed by a straightforward work-up to yield (**5**). The second step of the synthesis is another use of *n*-BuLi to extract a bromine atom, generating LiBr and an anion. This anion is subsequently protonated by water to generate (**6**). Again, the work-up for this reaction is straightforward and after recrystallization, yields a white solid that can be used as a starting material for the next step.

The final step to generate the target precursor involves the Petasis reaction. First reported in 1993 by N.A. Petasis, this reaction was originally intended to produce alkylidene cyclopropane derivatives by reacting biscyclopropyl titanocene with several types of carbonyls. In their paper, Petasis and Bzowej discuss the preparation of biscyclopropyl titanocene from titanocene dichloride and cyclopropyllithium; cyclopropropyllithium can be generated from cyclopropyl bromide and lithium metal. The biscyclopropyl titanocene is thermally unstable at room temperature, but can be stored at -20°C for an extended period of time.

Petasis and Bzowej further argue that the possibility for ß-elimination may result in the formation of a strained cyclopropene, and additionally, (**9**) has the possibility of undergoing isomerization to an allyl system. Nevertheless, they found that (**9**) exhibits olefinating activity and can react with carbonyl compounds to form various alkylidene cyclopropane derivatives. The procedure for their reaction is laid out in Scheme 4 below.

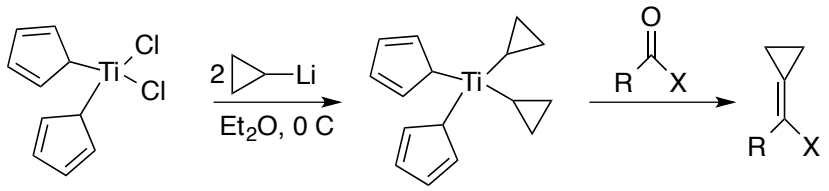

8 **9** **10**

Scheme 4. Generation of Biscylopropyl Titanocene (9) from Titanocene Dichloride (8) and Cyclopropyllithium. From here, the compound can react with any number of carbonyls to yield alkylidene cyclopropane derivatives (10).

For this study, (**6**) was first reacted with *t*-BuLi to extract the bromine atom and set up this site for reaction with the titanocene. Then, using titanocene dichloride and 2-adamantanone as the carbonyl compound, adamantane connected by a double bond was attached to the phenanthrene-based backbone. This resulted in the generation of the 2-adamantylidenecarbene precursor, (**7**).

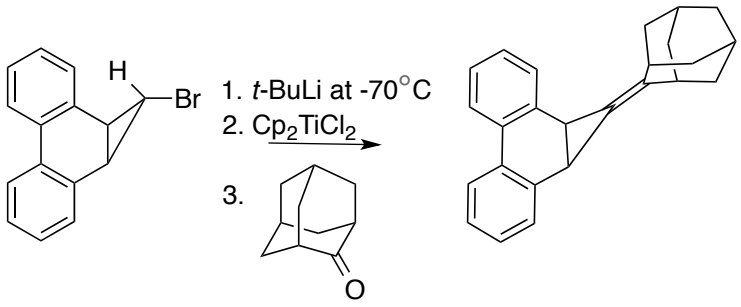

11

Scheme 5. Generation of the Target Precursor (7) via the Petasis Reaction Using Titanocene Dichloride and 2-Adamantanone (11).

Synthesis of the 2-Adamantylidenecarbene precursor

The target precursor (**7**) was prepared in a yield of 18.41% from (**6**), with a melting point of 140.4-146.6 °C. GCMS displayed the predicted *m/z* ratio, 324. The ^{1}H NMR displays the expected 25 protons. The eight aromatic protons appear as three signals from δ 7.20 to 7.95 ppm. However, two similar environments may be overlapping and accordingly, indistinguishable. Additionally, the two protons connected to the cyclopropyl ring appear as a singlet at δ 3.18 ppm. The remaining protons in the adamantane group are present further up-field, from δ 1.00 to 2.56 ppm. The ^{13}C NMR shows 19 carbon signals, as expected, since there is symmetry through the center of the phenanthrene-backbone. The four unique aromatic carbons are present between δ 123.15 and 128.53 ppm. IR stretches characteristic of alkanes were also present, seen between 2845 cm^{-1} and 2989 cm^{-1}. The peak at 1772 cm^{-1} may correspond to the C=C; it is a weak signal, as there is no large net change in the dipole moment. Additionally, a C-C stretch characteristic of aromatics is present at 1599 cm^{-1}.

X-Ray Crystallography

Sizable crystals were obtained through slow evaporation of fractions from the column chromatography, allowing the determination of structure by X-ray crystallographic analysis. The crystal structure of (**7**) is shown in Figure 13.

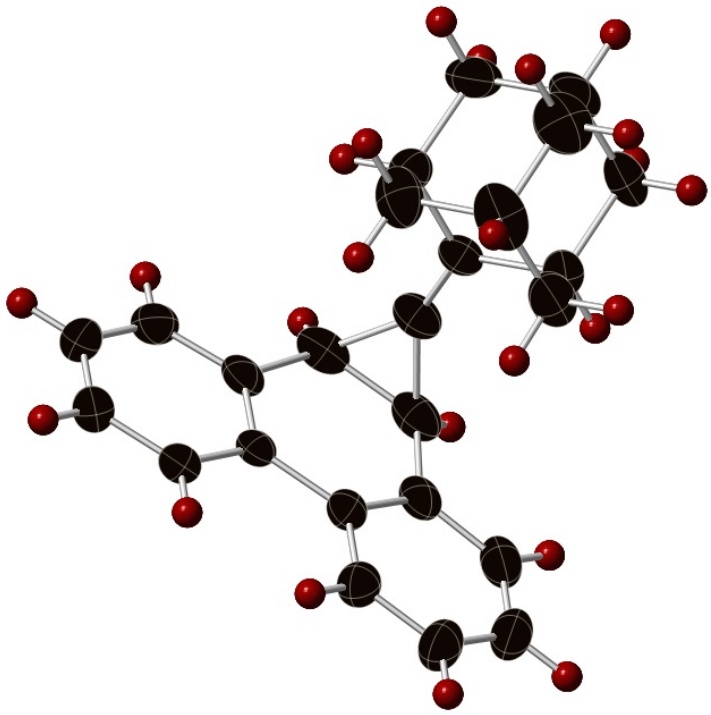

Figure 13. X-ray crystal structure of the target precursor

The crystal appeared clear and colorless. Its approximate dimensions measured 0.080 mm x 0.270 mm x 0.400 mm. This crystal is part of an orthorhombic system with a unit cell volume of 1775.1 $Å^3$. The unity cell contains four molecules. The phenanthrene backbone and cyclopropyl ring can clearly be seen, and there is a double bond present of length 1.313 $Å^3$.

Table 1. Crystallographic Data for the Target Precursor

Crystal System	Space Group	Unit Cell	Volume	Z	Density	R1[1>2σ(I)]
orthorombic	P 21 21 21	a= 6.23 Å, α= 90° b= 11.24 Å, β= 90° c= 25.35 Å, γ= 90°	1775.1 $Å^3$	4	1.218 g/cm^3	0.0424

2.2 Photolysis

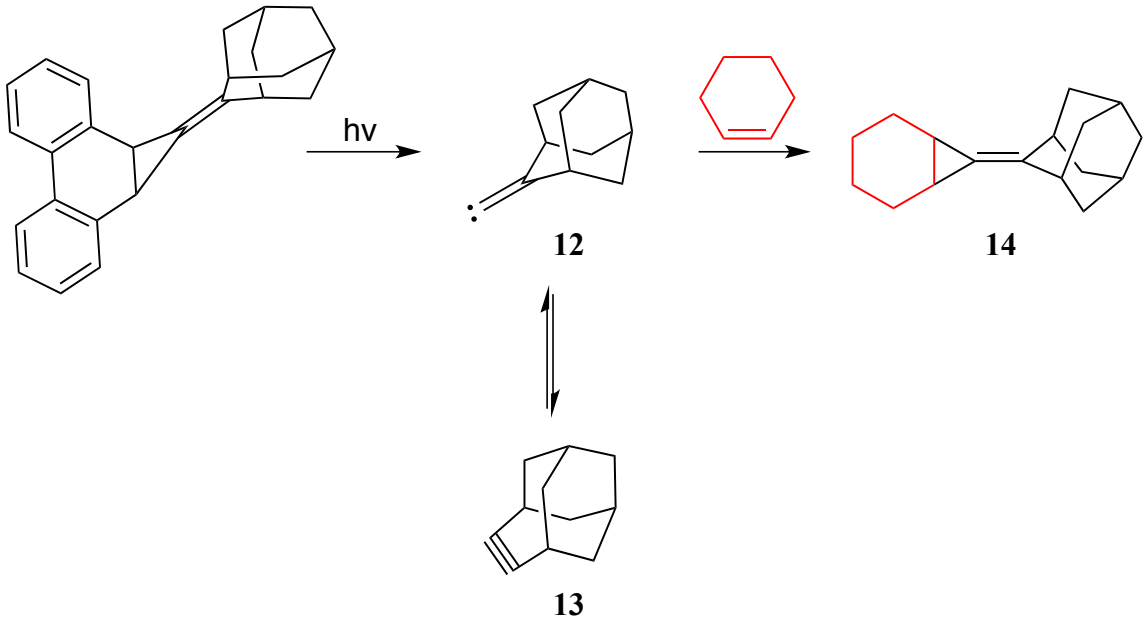

Scheme 5. Generation of 2-Adamantylidenecarbene (12) and Subsequent Trapping with Cyclohexene via Laser Flash Photolysis

Photolysis of the precursor (**7**) was carried out in cyclohexene at room temperature. Initially, the photolysis was monitored by GC/MS every hour until the starting material had been consumed. However, after 12 hours, the reaction was monitored at 4 hour-intervals. The consumption time of (**7**) was about 25 hours. The 2-adamantylidenecarbene **(12)** that was generated through photolysis was trapped with the cyclohexene, producing (**14**). The photolysis reaction and isomeric rearrangement are illustrated in Scheme 5. Looking at the ^{1}H NMR of (**14**), the similar nature of all of the proton signals resulted in a very cluttered spectrum. However, all of the signals appeared in the alkane region of the spectrum, consistent with the structure of the trapped product. The singlet at δ 2.67 ppm corresponds to the 2 hydrogens in the cyclopropyl ring. Furthermore, the aromatic shifts no longer appear on the spectrum, supporting the conclusion that 2-adamantylidenecarbene was generated, with the loss of the phenanthrene-

backbone, and subsequently trapped, generating (**14**). Most importantly, these data are consistent with the spectrum that Sasaki *et. al.* reported when they trapped 2-adamantylidenecarbene with cyclohexene, allowing us to confirm the successful generation and subsequent trapping of 2-adamantylidenecarbene. No evidence of 4-homoadamantyne, however, was observed.

Additionally, an isomer of the 2-adamantylidenecarbene precursor was produced. This occurred through a 1,5-alkyl shift, followed by an electrocyclic ring opening, resulting in the formation of a seven-membered ring. The mechanism of this reaction is also shown in Scheme 6.[24] The resulting isomer (**15**) did not photolyze and was present in the GC/MS after 25 hours, with an *m/z* of 324. Examination of the ^{1}H NMR further supported this conclusion. Seventeen signals are present, although there are eighteen unique proton environments in the isomer due to the aysmmetry of the backbone. Nevertheless, eight unique aromatic signals appear between δ 7.17 and 7.69 ppm, and the two protons in the double bond in the seven-membered ring appears as singlets at δ 6.67-6.72 and 6.52-6.55 ppm. The remaining signals up-field correspond to protons in the adamantane group.

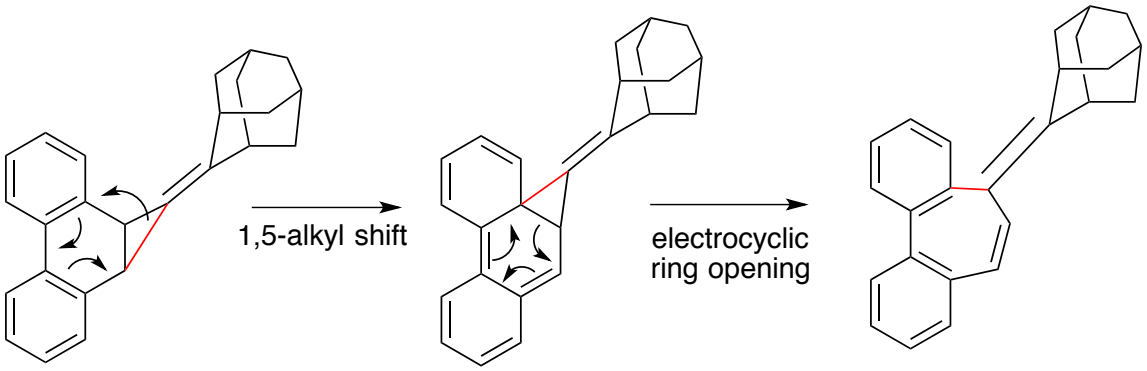

15

Scheme 6. Rearrangement of the 2-Adamantylidenecarbene Precursor (12)

2.3 Computational Studies

Geometry optimizations of 2-adamantylidenecarbene **(12)**, in both its singlet and triplet form, were performed using Gaussian at the B3LYP/6-31+G** level. After minimization using density functional theory (DFT), the single point energies of the two carbene species and 4-homoadamantyne were calculated using coupled cluster methods (CCSD(T)/cc-pVTZ. Frequency calculations of the minima and transition states were used to confirm the nature of these points; transition states have a single imaginary frequency, while the minima have no imaginary frequencies. The results are listed in Table 2.

Table 2. Computational Data

Species	DFT Energy (kcal/mol)	CCSD Energy (kcal/mol)
2-adamantylidenecarbene (singlet)	0	0
2-adamantylidenecarbene (triplet)	44.8	29.0
Transition State	26.6	24.7
4-Homoadamantyne	68.5	12.0

The difference in single point energies, ΔE, between the singlet and triplet carbene states is 29.0 kcal/mol, with the singlet state more energetically stable. A schematic of this energy difference is shown in Figure 14.

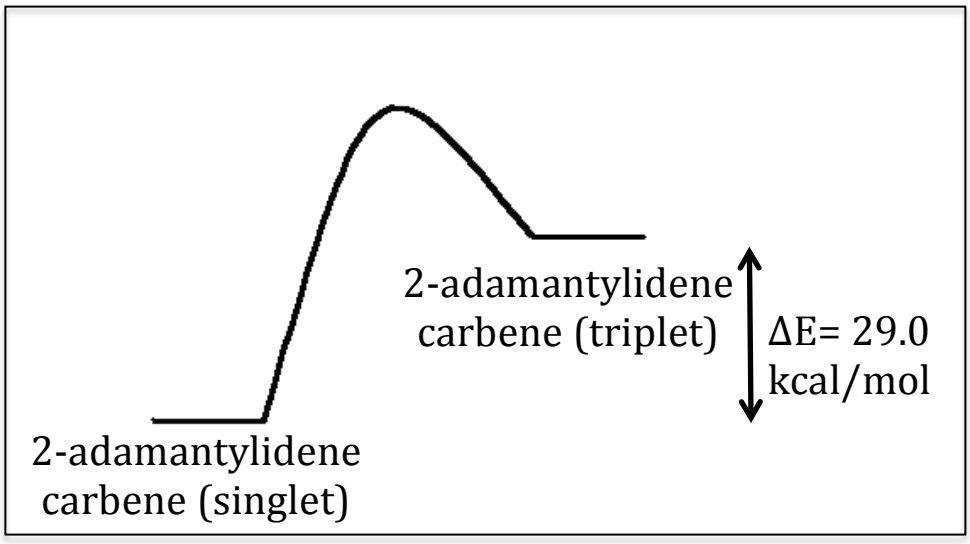

Figure 14. The difference in single point energies between the singlet and triplet states for 2-adamantylidenecarbene.

Additionally, the reaction from the singlet 2-adamantylidenecarbene to 4-homoadamantyne was examined. The transition barrier, $\Delta E^{\ddagger}$, was calculated to be +24.8 kcal/mol and the ΔE to be +12.0 kcal/mol, with the singlet carbene lower in energy. A visual of these values is seen in Figure 15.

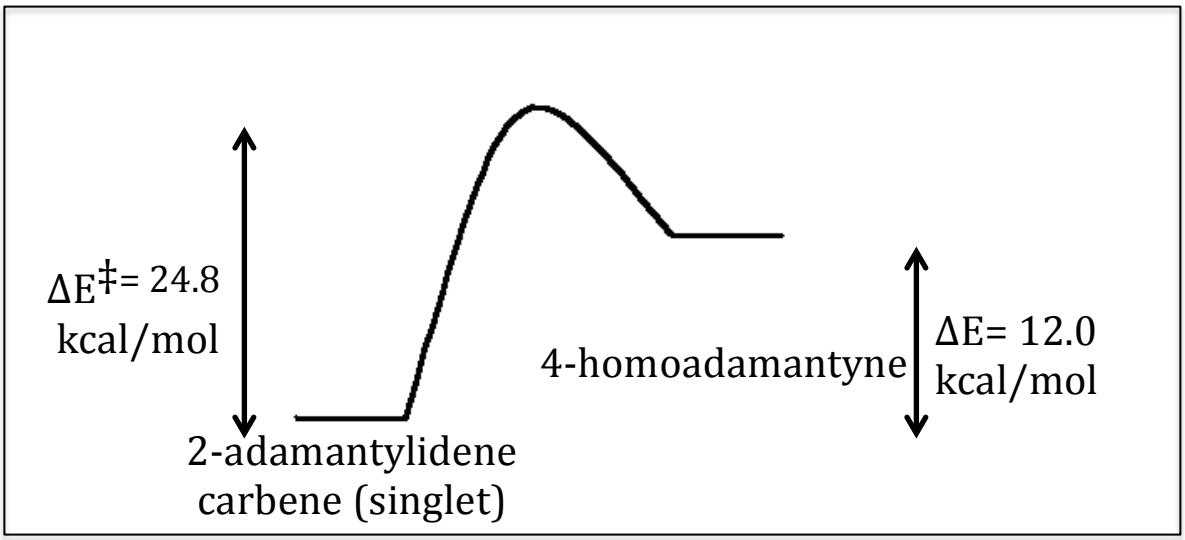

Figure 15. The difference in single point energies between the singlet 2-adamantylidenecarbene and 4-homoadamantyne, as well as the transition barrier.

Conclusion

This thesis demonstrated that 2-adamantylidenecarbene can, in fact, be generated through photolytic cleavage of a phenanthrene-based precursor. This precursor (**7**) was synthesized through a three-step procedure, beginning with phenanthrene. After generating the dibromo carbene and then the monobromo compound, the Petasis reaction was utilized in order to attach 2-adamantanone, (**11**), to the phenanthrene-based backbone, producing the target precursor (**7**). The precursor was characterized by analytical techniques including GC/MS, ^{1}H NMR, ^{13}C NMR, and IR. The crystal structure for the 2-adamantylidenecarbene precursor verified the spectral data obtained for this compound.

This precursor was photolyzed, producing (**12**) and subsequently trapped with cyclohexene to generate (**14**). We concluded that the 2-adamantylidenecarbene had successfully been trapped, as the ^{1}H NMR was consistent with the spectral data that Sasaki *et. al.* reported for the same experiment. A rearrangement of the precursor was also observed, and this isomer, (**15**), did not photolyze.

Additionally, computational studies showed that the singlet 2-adamantylidenecarbene is more energetically favorable than both the triplet state and 4-homoadamantyne, by 29.0 kcal/mol and 12.0 kcal/mol, respectively. The transition barrier between the singlet and 4-homoadamantyne was calculated to be 24.8 kcal/mol.

In the future, further studies should be performed in order to completely characterize this trapped product, (**14**); this includes ^{13}C NMR, IR, and X-ray crystallography. In addition, the possible ring expansion to 4-homoadamantyne (**13**) could be further examined.

Experimental

4.1 General Comments

Standard synthetic techniques were employed for each step with commercially available starting materials and solvents. Reactions requiring anhydrous conditions were carried out under argon using oven-dried equipment. Tetrahydrofuran was dried by passage through two alumina packed columns (2' x 4").

Gas chromatography-mass spectrometry (GC/MS) analysis was performed on an Agilent Technologies 7890A GC System and 5975C insert MSD with Triple-Axis Detector. ^{1}H NMR and ^{13}C NMR were taken at 500 MHz and 125 MHz, respectively, using a Bruker Avance 400 spectrometer. IR spectra were recorded on a Mattson 4020 Galaxy Series FT-IR (2500-400 cm^{-1}). Column chromatography was performed with a 120 mesh silica gel. Photolysis was performed in a Rayonet Photochamber (λ= 254 – 419nm) at 250 watts.

4.2 Synthetic Procedurs

Preparation of 1,1-Dibromo-1a-dihydrocyclopropa[*l*]phenanthrene (5)

Phenanthrene (35.6 g, 0.2 mol), benzyltriethylammonium chloride (0.5 g, 0.002 mol), $CHBr_3$ (40 mL, 116 g, 0.46 mol), CH_2Cl_2 (40 mL), and EtOH (1 mL) were combined in a 500 mL Erlenmeyer flask containing a dumb-bell shaped stir bar. Aqueous 50% NaOH (80 mL) was added to the mixture in approximately 5 mL increments over 30 minutes. The flask was loosely stoppered and the mixture was allowed to stir for four days at room temperature. The mixture, which appeared frothy at first, became a thick, brown sludge after four days. The contents were poured into a 500 mL separatory funnel. The flask was rinsed with CH_2Cl_2 (100 mL) and H_2O (100 mL). The rinses were added to the separatory funnel and after shaking, the aqueous and organic layers separated. The aqueous layer was extracted with CH_2Cl_2 (2 x 50 mL). All of the

organic components of the mixture were combined and then washed with 2 M HCl (2 x 100 mL), H_2O (2 x 100 mL), and brine (1 x 100 mL). Vacuum filtration produced a light brown solid, which was subsequently recrystallized by dissolving in $CHCl_3$ and heating the mixture to roughly 80 °C until the crystals were no longer visible. Carbon black was added to this solution, and gravity filtration was then performed. Vacuum filtration of the recrystallized product resulted in a white solid (10.5 g). Concentration of the filtrate from the first vacuum filtration yielded an additional crop (1.14 g), which was also recrystallized. The combined yield was 11.64 g (16.72%).

^{1}H NMR ($CDCl_3$) δ 8.70-8.72 (d, 4H), 8.01-8.03 (dd, 1H), 7.90-7.92 (dd, 5H), 7.76 (s, 5H), 7.60-7.65 (m, 10H), 7.46-7.50 (ddd, 2H), 7.39-7.42 (dtd, 2H), 3.41 (s, 2H).

Preparation of 1-Bromo-1a-dihydrocyclopropa[*l*]phenanthrene (6)

In an oven-dried 250 mL round-bottomed flask containing a stir bar, under an inert atmosphere of argon, 10.47 g of (**5**) was dissolved in 150 mL dry THF. This mixture was cooled to -70 °C using a dry ice and acetone bath. 13 mL *n*-butyllithium (2.5M, 32.5 mmol) was added drop-wise over 20 minutes using a 20 mL syringe, all the while ensuring that the temperature of the solution did not rise above -60 °C. The solution gradually turned dark green, indicating that the starting material had reacted with the reagent. The reaction stirred for one hour at this temperature, and then 50 mL H_2O was added with a 10 mL syringe. Once the solution reached -20 °C, the dry ice and acetone bath was lowered and replaced by a water and regular ice bath. After one hour, this ice bath was removed and the solution was allowed to stir overnight at room temperature. The reaction mixture was then transferred to a 500 mL separatory funnel, and upon

shaking, the organic and aqueous layers separated. The aqueous layer was extracted with ether (2 x 50 mL). The combined organic layers were washed with H_2O (2 x 50 mL) and brine (1 x 50 mL). GC/MS was performed on approximately 1 *u*L of product to verify that the reaction had run to completion. The organic product was allowed to sit over night at room temperature in order for the solvent to evaporate. The following day, the solid was recrystallized by dissolving it in $CHCl_3$ and heating the mixture to roughly 80 °C until the crystals dissolved. Carbon black was added to this solution, and gravity filtration was then performed. Vacuum filtration of the recrystallized product resulted in a white solid of 2.70 g (32.99%). ^{1}H NMR ($CDCl_3$) δ 7.95-7.97 (dd, 9H), 7.49-7.71 (dd, 9H), 7.42 (m, 1H), 7.28-7.34 (m, 11H), 3.02-3.03 (d, 8H), 2.42-2.44 (m, 4H).

Preparation of the Target Precursor (7) via the Titanocene Reaction

In an oven-dried 250 mL round-bottomed flask attached to a condenser and containing a stir bar, under an inert atmosphere, 2.70 g of (**6**) was dissolved in 60 mL dry THF at room temperature. The mixture was then cooled to -75 °C using a dry ice and acetone bath. 13 mL of room-temperature *tert*-butyllithium was added drop-wise over 10 minutes using a 10 mL syringe (7 mL + 6 mL). During this addition, the temperature of the mixture was kept between -75 °C and -65 °C. The reaction was allowed to sit at this temperature for 30 minutes. Following this, 1.105 g (4 mmol) bis(cyclopentadienyl)titanium(IV)dichloride was added to the dark green mixture. After five minutes, the dry ice and acetone ice bath was switched out for a water and regular ice bath. Once the temperature warmed to 0°C, the mixture was allowed to sit at this temperature for 90 minutes. Then, 2.00 g (13.3 mmol) of 2-adamantanone was added to the mixture. A reflux was set up at 65 °C with the solution stirring for 24 hours. The product was

subsequently poured into a 100 mL beaker. The round-bottomed flask was washed with ether (50 mL) and 1 mL of the product was added to a test tube. The test tube was washed with H_2O (1 mL) and dried with sodium sulfate. GC/MS was performed on approximately 1 *u*L of aliquot sample.

Column chromatography yielded clear crystals, and the appropriate fractions containing the 2-adamantylidenecarbene precursor were combined into one 400 mL beaker by rinsing the test tubes with CH_2Cl_2. After allowing the CH_2Cl_2 to slowly evaporate, these combined fractions were recrystallized in a vial by adding hexanes and heating the mixture until the white specks disappeared. Recrystallization yielded 497 mg (18.41%) of a pure white solid. ^{1}H NMR ($CDCl_3$) δ 7.92-7.96 (m, 2H), 7.36-7.38 (m, 2H), 7.20-7.23 (m, 4H), 3.18 (s, 2H), 2.56-2.57 (M, 2H), 1.93-1.96 (p, 1H), 1.81-1.84 (t, 4H), 1.70 (s, 2H), 1.62-1.65 (p, 1H), 1.52-1.54 (q, 3H), 1.00-1.02 (d, 2H); ^{13}C NMR ($CDCl_3$) δ 21.82, 28.19, 28.24, 36.23, 37.15, 38.60, 38.92, 77.20, 106.48, 106.74, 112.47, 123.15, 127.50, 128.53, 138.41, 141.42, 176.32, 211.08, 211.35

4.3 The Photolysis Experiment

The typical photolysis experiment consisted of the following procedure. 497 mg of precursor (**7**) were weighed out and dissolved in cyclohexene. 5 mL C_6D_6 was added to the vial, and the sample was degassed by bubbling dry argon for approximately one minute. The photolysis was monitored by GC/MS at one-hour intervals for the first 12 hours, then at four-hour intervals for the remainder of the reaction; the photolysis would continue as long as there was starting material in the reaction tube. The complete consumption of starting material, to our GC/MS sensitivity, was 25 hours. Following photolysis, a ^{1}H NMR spectrum was obtained and compared to the pre-photolysis spectrum.

4.4 X-Ray Crystallography

A clear colorless plate-like specimen of $C_{25}H_{25}$, approximate dimensions 0.080 mm x 0.270 mm x 0.400 mm, was used for the X-ray crystallographic analysis. The X-ray intensity data were measured.

The total exposure time was 15.41 hours. The frames were integrated with the Bruker SAINT software package using a narrow-frame algorithm. The integration of the data using an orthorhombic unit cell yielded a total of 14935 reflections to a maximum θ angle of 26.38° (0.80 Å resolution), of which 3610 were independent (average redundancy 4.137, completeness = 99.7%, R_{int} = 2.85%, R_{sig} =2.32%) and 3256 (90.19%) were greater than $2\sigma(F^2)$. The final cell constants of $\underline{a}$ = 6.2276(7) Å, $\underline{b}$ = 11.2427(13) Å, $\underline{c}$ = 25.353(3) Å, volume = 1775.1(4) $Å^3$, are based upon the refinement of the XYZ-centroids of 5082 reflections above 20 σ(I) with 4.842° < 2θ < 52.49°. Data were corrected for absorption effects using the multi-scan method (SADABS). The ratio of minimum to maximum apparent transmission was 0.832. The calculated minimum and maximum transmission coefficients (based on crystal size) are 0.9730 and 0.9950.

The final anisotropic full-matrix least-squares refinement on F^2 with 226 variables converged at R1 = 4.24%, for the observed data and wR2 = 13.34% for all data. The goodness-of-fit was 1.024. The largest peak in the final difference electron density synthesis was 0.201 $e^-/Å^3$ and the largest hole was -0.136 $e^-/Å^3$ with an RMS deviation of 0.036 $e^-/Å^3$. On the basis of the final model, the calculated density was 1.218 g/cm^3 and F(000), 700 e^-.

1,1-Dibromo-1a-dihydrocyclopropa[*l*]phenanthrene (**5**)
starting phenanthrene= 35.6g
Yield= 11.64 g, 16.72%
^{1}H NMR ($CDCl_3$) δ 8.70-8.72 (d, 4H), 8.01-8.03 (dd, 1H), 7.90-7.92 (dd, 5H), 7.76 (s, 5H), 7.60-7.65 (m, 10H), 7.46-7.50 (ddd, 2H), 7.39-7.42 (dtd, 2H), 3.41 (s, 2H)

1-Bromo-1a-dihydrocyclopropa[*l*]phenanthrene (**6**)
starting 1,1-Dibromo-1a-dihydrocyclopropa[*l*]phenanthrene= 10.47g
Yield= 2.70 g, 32.99%
^{1}H NMR ($CDCl_3$) δ 7.95-7.97 (dd, 9H), 7.49-7.71 (dd, 9H), 7.42 (m, 1H), 7.28-7.34 (m, 11H), 3.02-3.03 (d, 8H), 2.42-2.44 (m, 4H)

2-Adamantylidenecarbene Precursor (**7**)
starting 1,1-Dibromo-1a-dihydrocyclopropa[*l*]phenanthrene= 2.70 g
Yield= 497 mg, 18.41%
mp: 140.4-146.6 °C
^{1}H NMR ($CDCl_3$) δ 7.92-7.96 (m, 2H), 7.36-7.38 (m, 2H), 7.20-7.23 (m, 4H), 3.18 (s, 2H), 2.56-2.57 (M, 2H), 1.93-1.96 (p, 1H), 1.81-1.84 (t, 4H), 1.70 (s, 2H), 1.62-1.65 (p, 1H), 1.52-1.54 (q, 3H), 1.00-1.02 (d, 2H)
^{13}C NMR ($CDCl_3$) δ 21.82, 28.19, 28.24, 36.23, 37.15, 38.60, 38.92, 77.20, 106.48, 106.74, 112.47, 123.15, 127.50, 128.53, 138.41, 141.42, 176.32, 211.08, 211.35

Trapped Product (**14**)
^{1}H NMR ($CDCl_3$) δ 2.67 (s), 2.14-2.17 (d), 1.98 (s), 1.82-1.92 (dd), 1.79 (s), 1.72-1.77 (dt), 1.54-1.57 (d), 1.45-1.47 (d), 1.36-1.40 (d), 1.23-1.32 (dp), 1.11-1.15 (m). The overlapping peaks makes it difficult to distinguish the number of protons in each environment.

Adamatylidenecarbene Precursor Isomer (**15**)
^{1}H NMR ($CDCl_3$) δ 7.64-7.69 (m, 1H), 7.56 (s, 1H), 7.35-7.39 (m, 1H), 7.32-7.35 (td, 2H), 7.27-7.30 (m, 2H), 7.17 (s, 1H), 6.67-6.72 (dd, 1H), 6.52-6.55 (dd, 1H), 2.96-2.98 (m, 1H), 2.78-2.79 (d, 1H), 2.02-2.05 (d, 2H), 1.92-1.97 (m, 3H), 1.82-1.86 (m, 1H), 1.80 (s, 3H), 1.59-1.63 (m, 1H), 1.45-1.47 (d, 1H), 1.30-1.32 (d, 1H)

References

[1] Kirmse, Wolfgang. *Carbene Chemistry*. Vol. 1. New York: Academic, 1964. Print.

[2] J.B. Dumas, *Ann. chim. phys*. [2] **58**, 28 (1835).

[3] H.V. Regnault, *Ann. chim. phys*. [2] **71**, 427 (1839).

[4] A. Perrot, *Ann. d. Chem*. **101**, 375 (1857).

[5] A.M. Butlerov, *Ann. d. Chem*. **120,** 356 (1861).

[6] J.U. Nef, *Ann. d. Chem*. **298**, 202 (1897).

[7] H. Staudinger and O. Kupfer, *Ber. deut. chem. Ges*. **44**, 2197 (1911); **45**, 501 (1912).

[8] H. Staudinger and R. Endle, *Ber. deut. chem. Ges*. **46**, 1437 (1913).

[9] H. Staudinger and J. Goldstein, *Ber. deut. chem. Ges*. **49**, 1923 (1916).

[10] H. Staudinger, E. Anthes, and F. Pfenninger, *Ber. deut. chem. Ges*. **29**, 1928 (1916).

[11] Arduengo, A; Harlow, R; Kline, M. *J. Am. Chem. Soc*. **113,** 361-363 (1991).

[12] B.S. Rabinovitch, E. Tsuikow-Roux, and E.W. Schlag, *J. Am. Chem. Soc*. **81,** 1081 (1989).

[13] H.M. Frey, *Proc. Roy. Soc*. **A251**, 575 (1959).

[14] J. Hine, *J. Am. Chem. Soc*. **72**, 2438 (1950).

[15] B.S. Rabinovitch and D.W. Setser, *J. Am. Chem. Soc*. **55**, 4329 (1933); **56**, 2381 (1934).

[16] K.S. Graves, D.M. Thamattoor and P.R. Rablen, *J. Org. Chem*., **2011**, 76: 1584.

[17] R.A. Farlow, D.M. Thamattoor, R.B. Sunoj and C.M. Hadad, *J. Org. Chem*., **2001**, 67: 3257.

[18] D.M. Thamattoor, J.R. Snoonian, H.M.Sulzbach and C.M. Hadad, *J. Org.Chem*, **1999**, 64: 5886.

[19] K.A. Moore, J.S. Vidaurri and D.M. Thamattoor, *J. Am. Chem Soc*., **2012**, 134: 20037.

[20] D.P. Maurer and D.M. Thamattoor, unpublished results

[21] Sasaki, T.; Eguchi, S.; Nakata, F. *Tetrahedron Lett*. **1978**; 19(23): 1999-2002.

[22] Sasaki, T.; Eguchi, S.; Tanida, M., Nakata, F., Esaki, T. *J. Org. Chem*. **1983;** *48*: 1579-1586.

[23] Komatsu, K.; Tsuji, R.; Masuda, H.; Takeuchi, K. *J. Chem. Soc., Chem. Commun*. **1991**; 71-72.

[24] Tobe, Y.; Iwasa, N.; Umeda, R.; Sonoda, M.; *Tetrahedron Lett*. **2001**; 42: 5485-5488

Vitae

Christine Elizabeth Wamsley
December 6, 1993
Ridgewood, New Jersey

Class of 2011
Ridgewood High School
Ridgewood, New Jersey

Class of 2015
Chemistry: Biochemistry and German Studies
Colby College
Waterville, Maine

APPENDIX: SPECTRAL DATA

Table of Contents

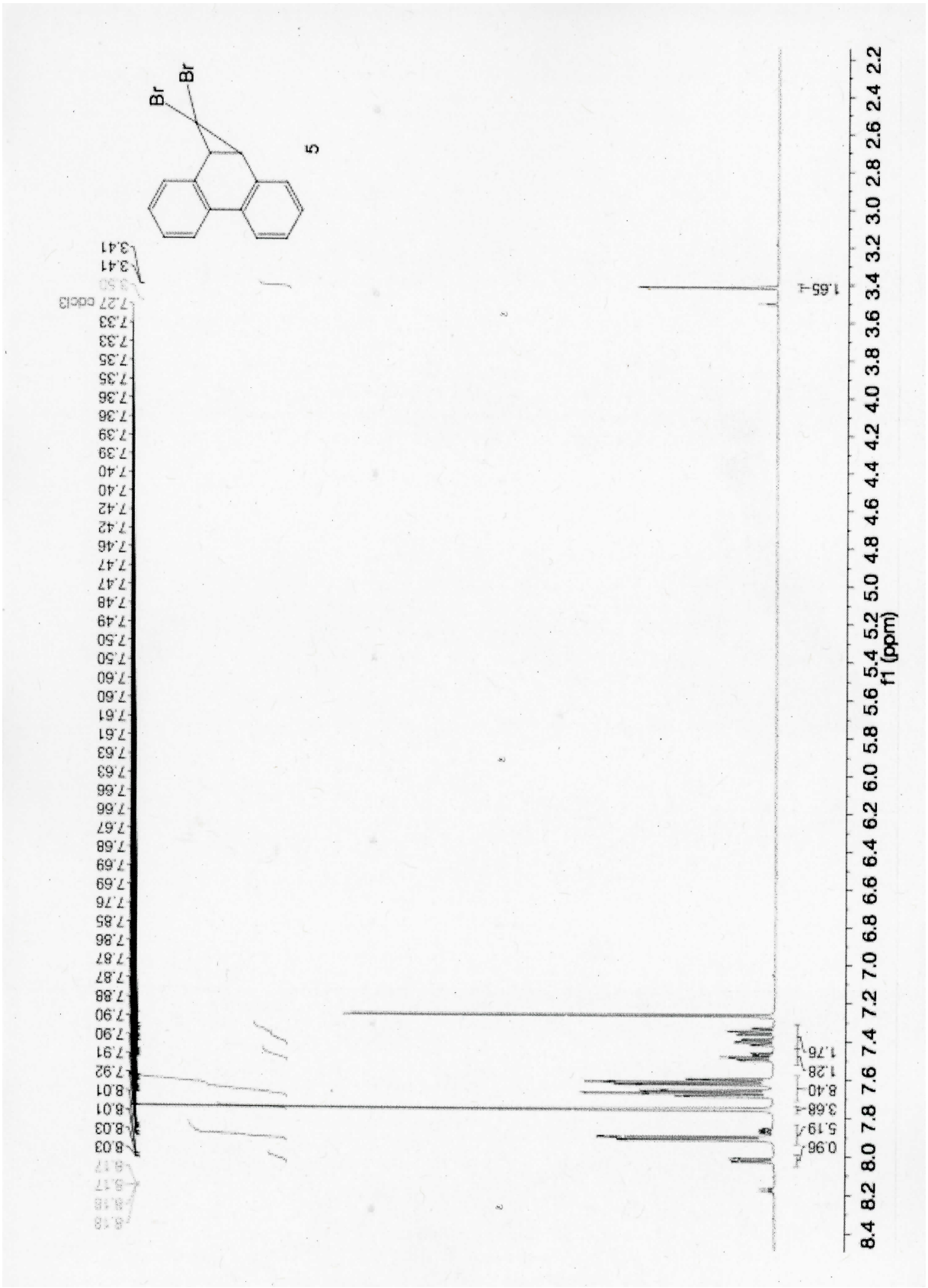
Br
Br
5
f1 (ppm)

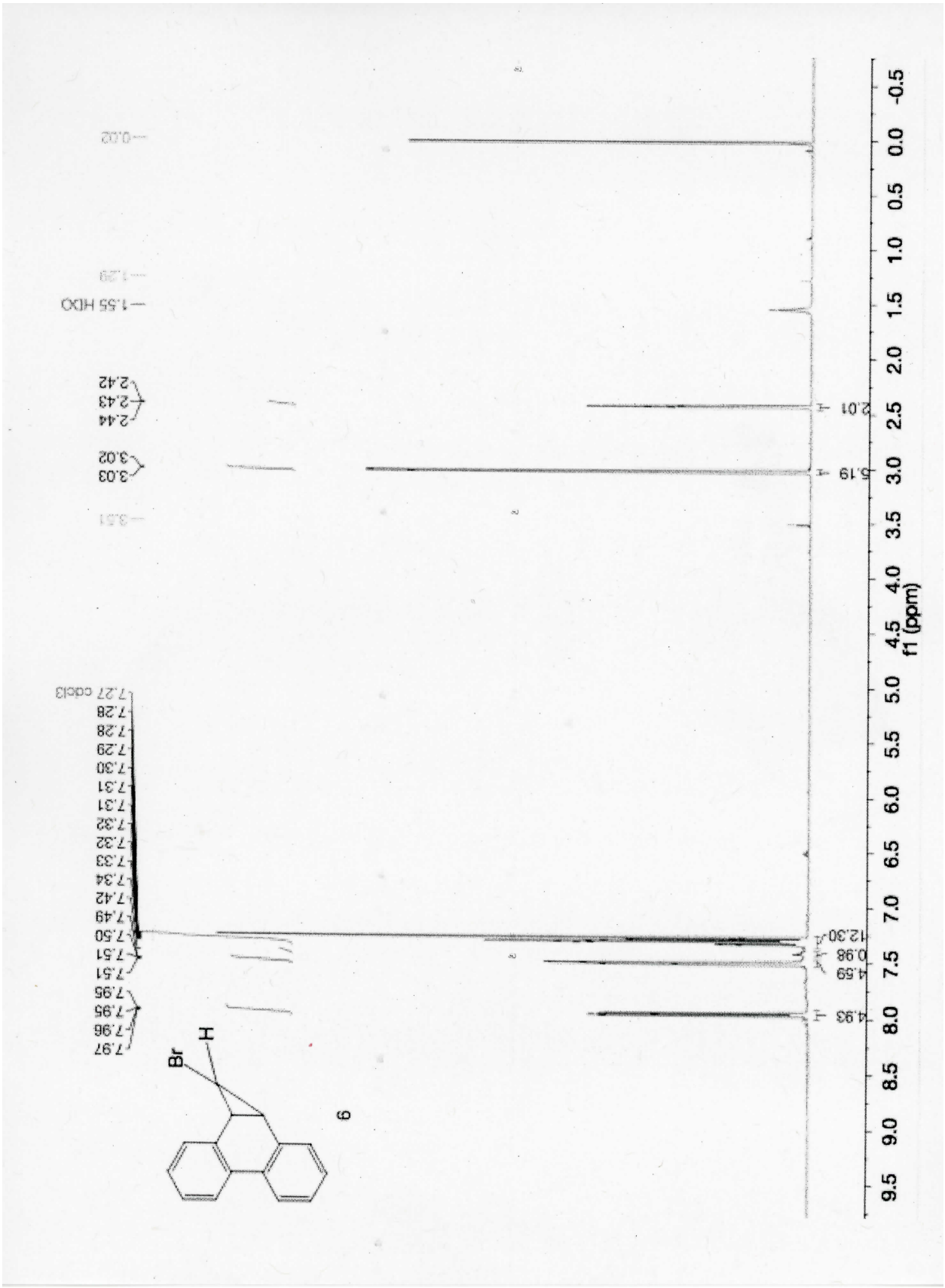
Br
H
9
f1 (ppm)

```
File       :D:\1\data\Christine\Snapshot\CW010815001.D
Operator   : Christine
Acquired   :  8 Jan 2015  16:11     using AcqMethod DASLAB3MIN.M
Instrument :    GCMS1
Sample Name: monobromo
Misc Info  : checking purity
Vial Number: 1
```

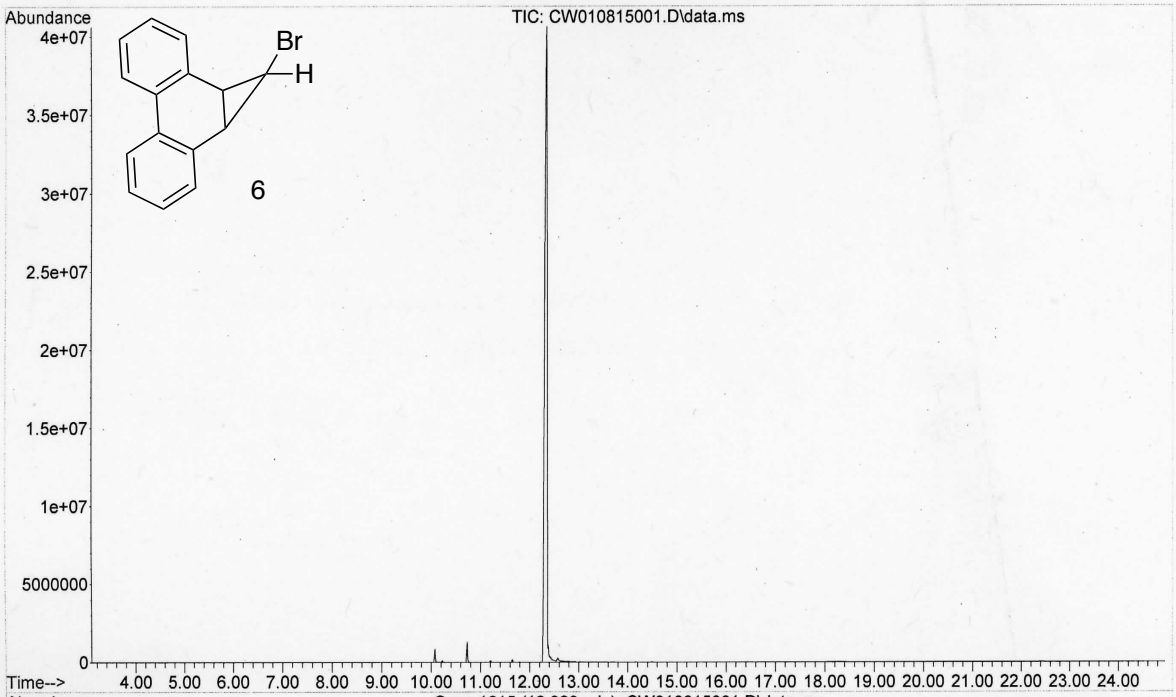

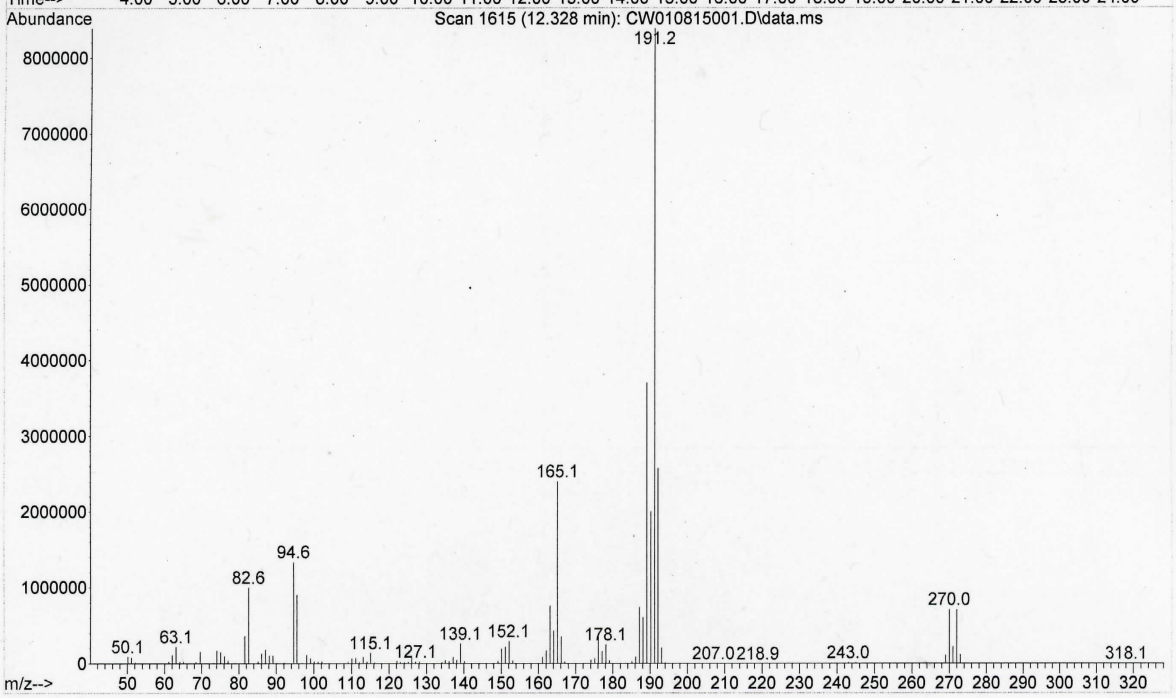

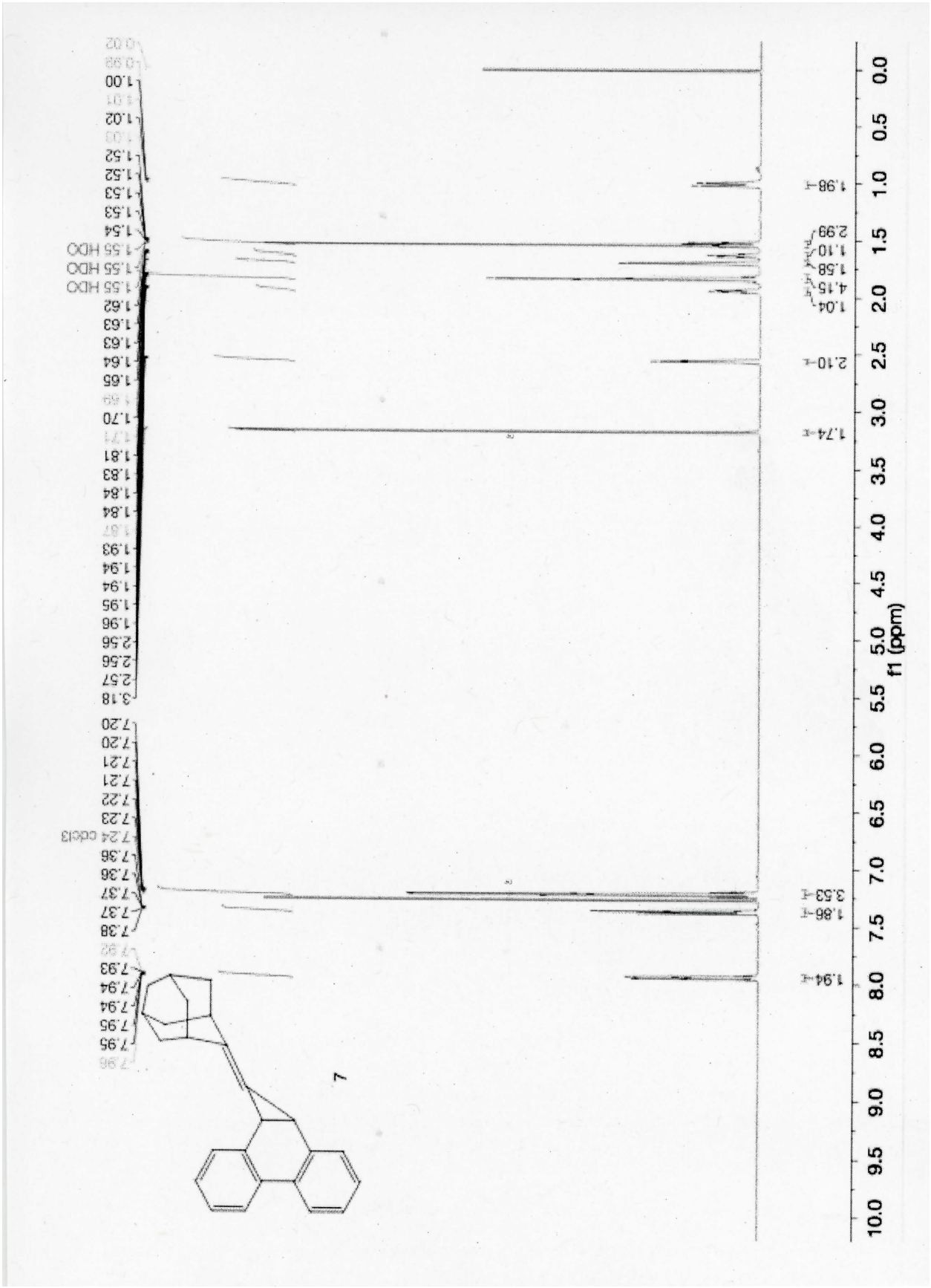
7
f1 (ppm)
CDCl3

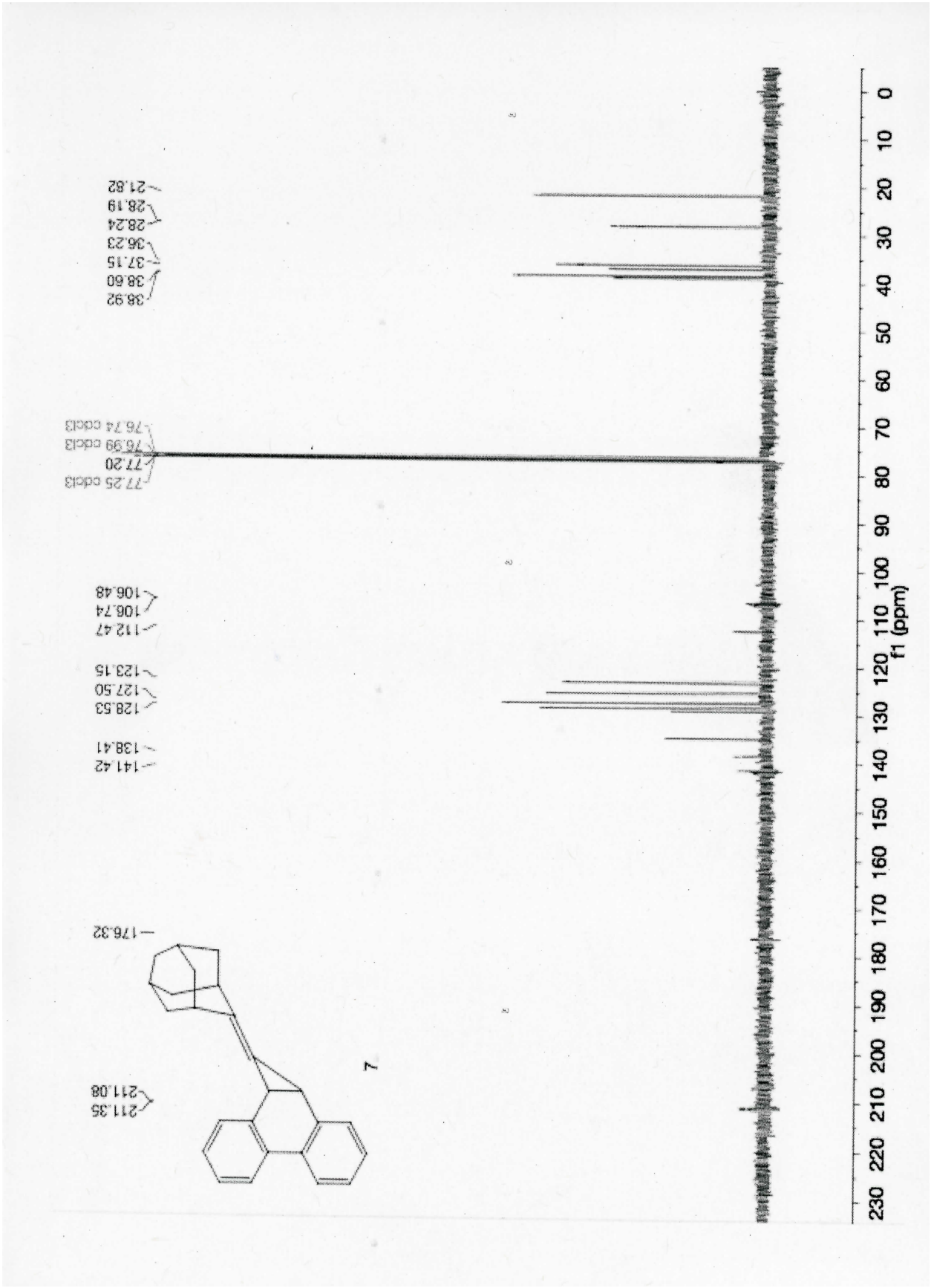
211.35
211.08
176.32
141.42
138.41
128.53
127.50
123.15
112.47
106.74
106.48
77.25 cdcl3
77.20
76.99 cdcl3
76.74 cdcl3
38.92
38.60
37.15
36.23
28.24
28.19
21.82
7
f1 (ppm)

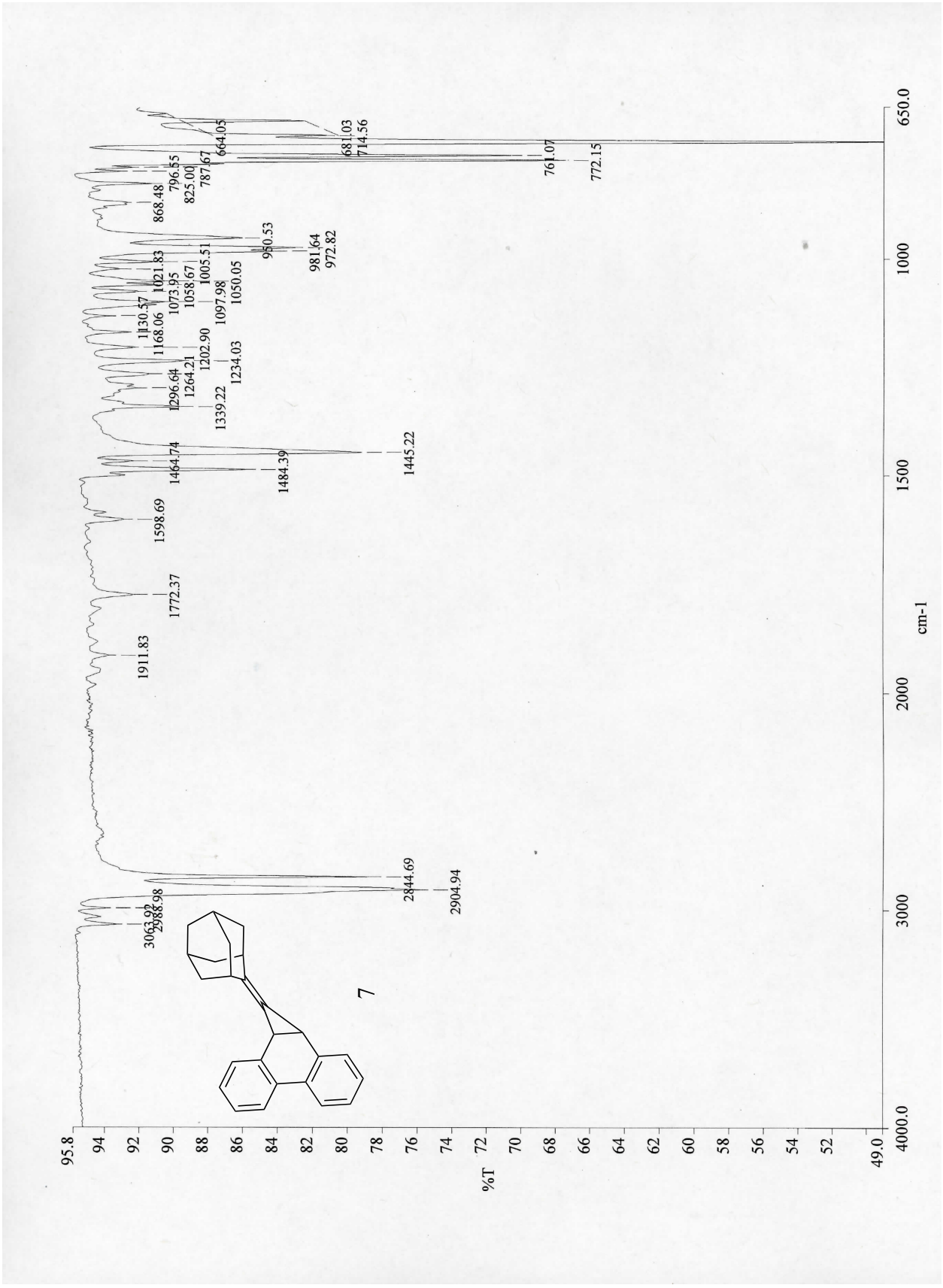
95.8
94
92
90
88
86
84
82
80
78
76
74
72
70
68
66
64
62
60
58
56
54
52
49.0
%T
4000.0
3000
2000
1500
1000
650.0
cm-1
3063.92
2988.98
2844.69
2904.94
1911.83
1772.37
1598.69
1464.74
1484.39
1445.22
1339.22
1296.64
1264.21
1234.03
1202.90
1168.06
1130.57
1097.98
1073.95
1058.67
1050.05
1021.83
1005.51
980.53
981.64
972.82
868.48
825.00
796.55
787.67
761.07
772.15
714.56
681.03
664.05
7

File :D:\1\data\Christine\CW110414004.D
Operator : Christine
Acquired : 4 Nov 2014 17:41 using AcqMethod DASLAB2MIN.M
Instrument : GCMS1
Sample Name: adamantilydene prec
Misc Info : recrystallized
Vial Number: 1

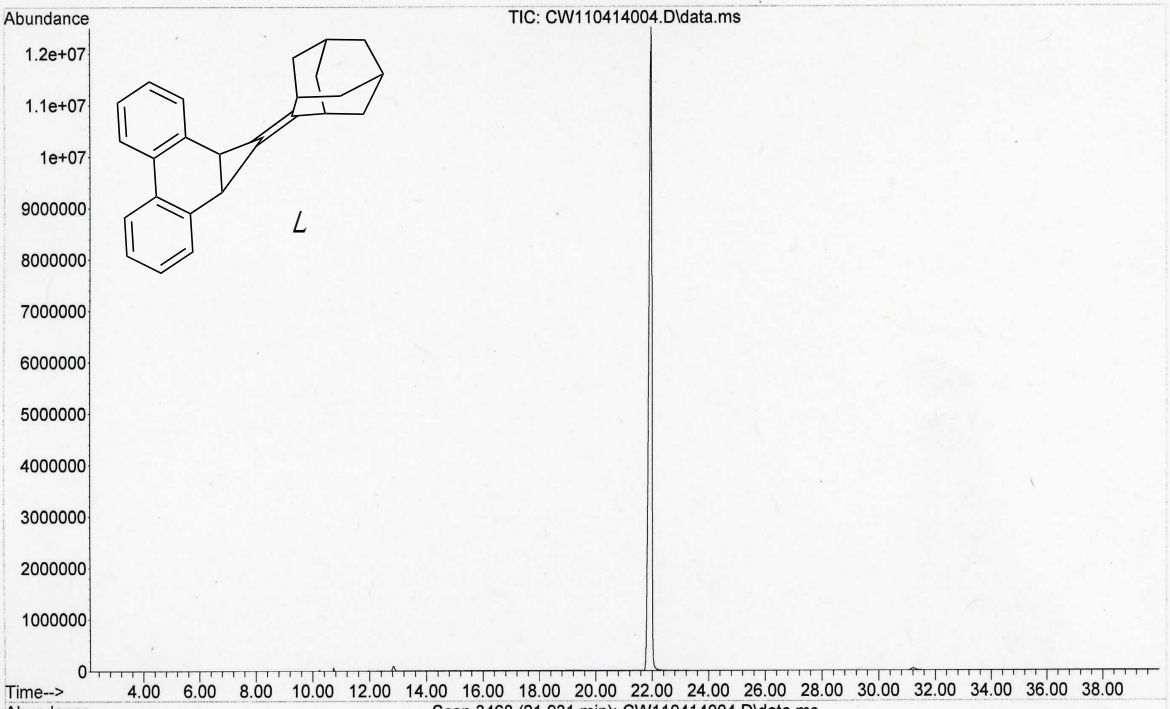

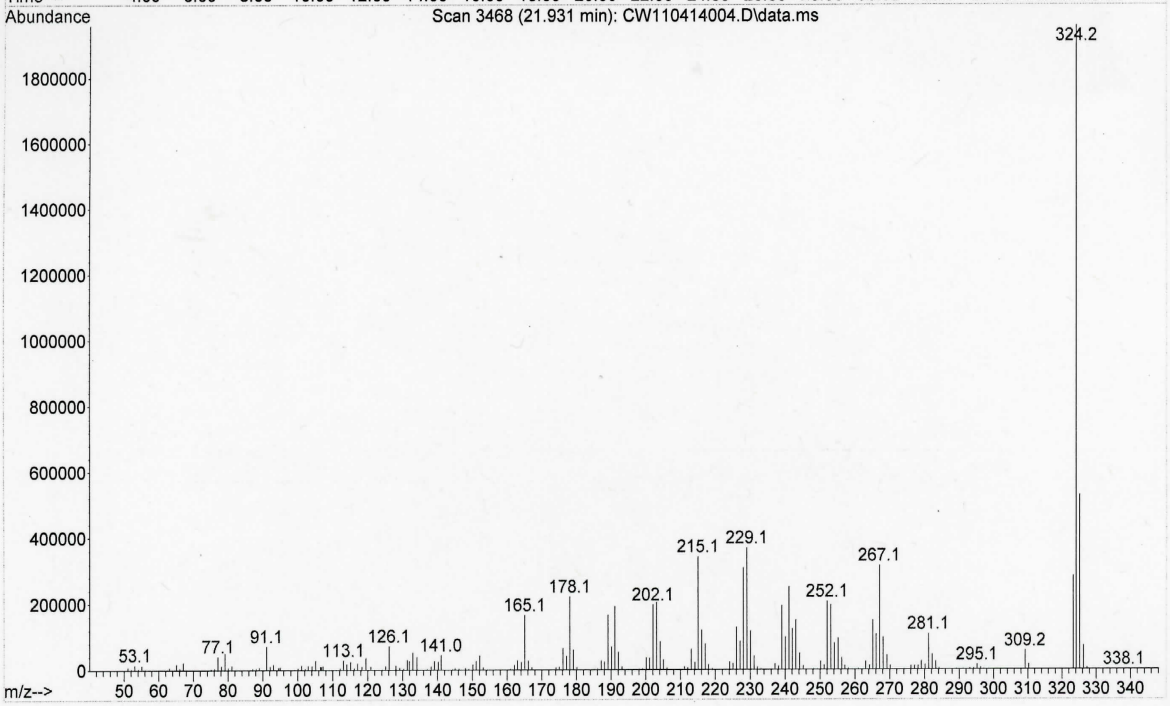

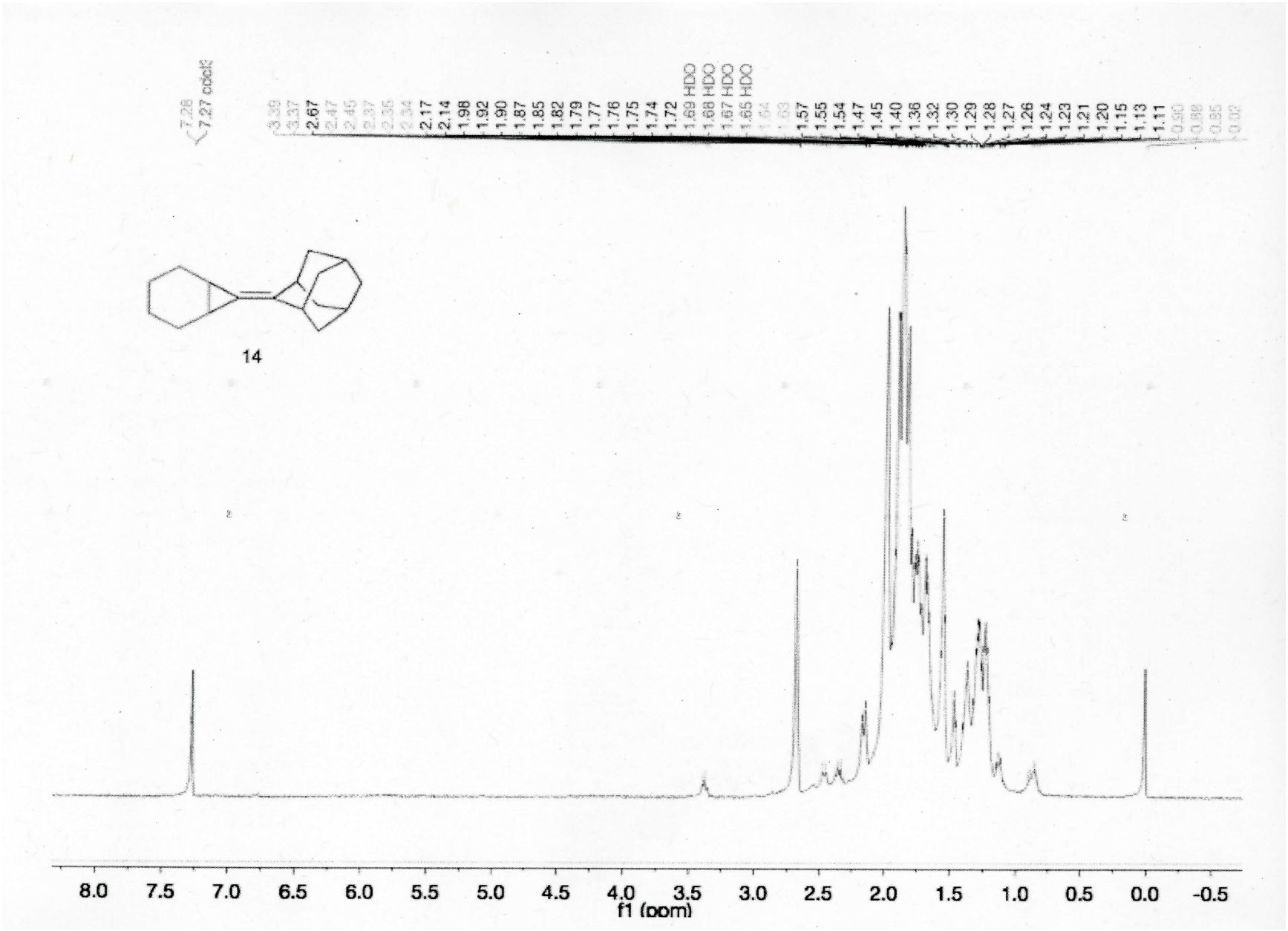
7.26
7.27 cdcl3
3.39
3.37
2.67
2.47
2.45
2.37
2.35
2.34
2.17
2.14
1.98
1.92
1.90
1.87
1.85
1.82
1.79
1.77
1.76
1.75
1.74
1.72
1.69 HDO
1.68 HDO
1.67 HDO
1.65 HDO
1.57
1.55
1.54
1.47
1.45
1.40
1.36
1.32
1.30
1.29
1.28
1.27
1.26
1.24
1.23
1.21
1.20
1.15
1.13
1.11
0.90
0.88
0.85
0.83
14
8.0
7.5
7.0
6.5
6.0
5.5
5.0
4.5
4.0
3.5
3.0
2.5
2.0
1.5
1.0
0.5
0.0
-0.5
f1 (ppm)

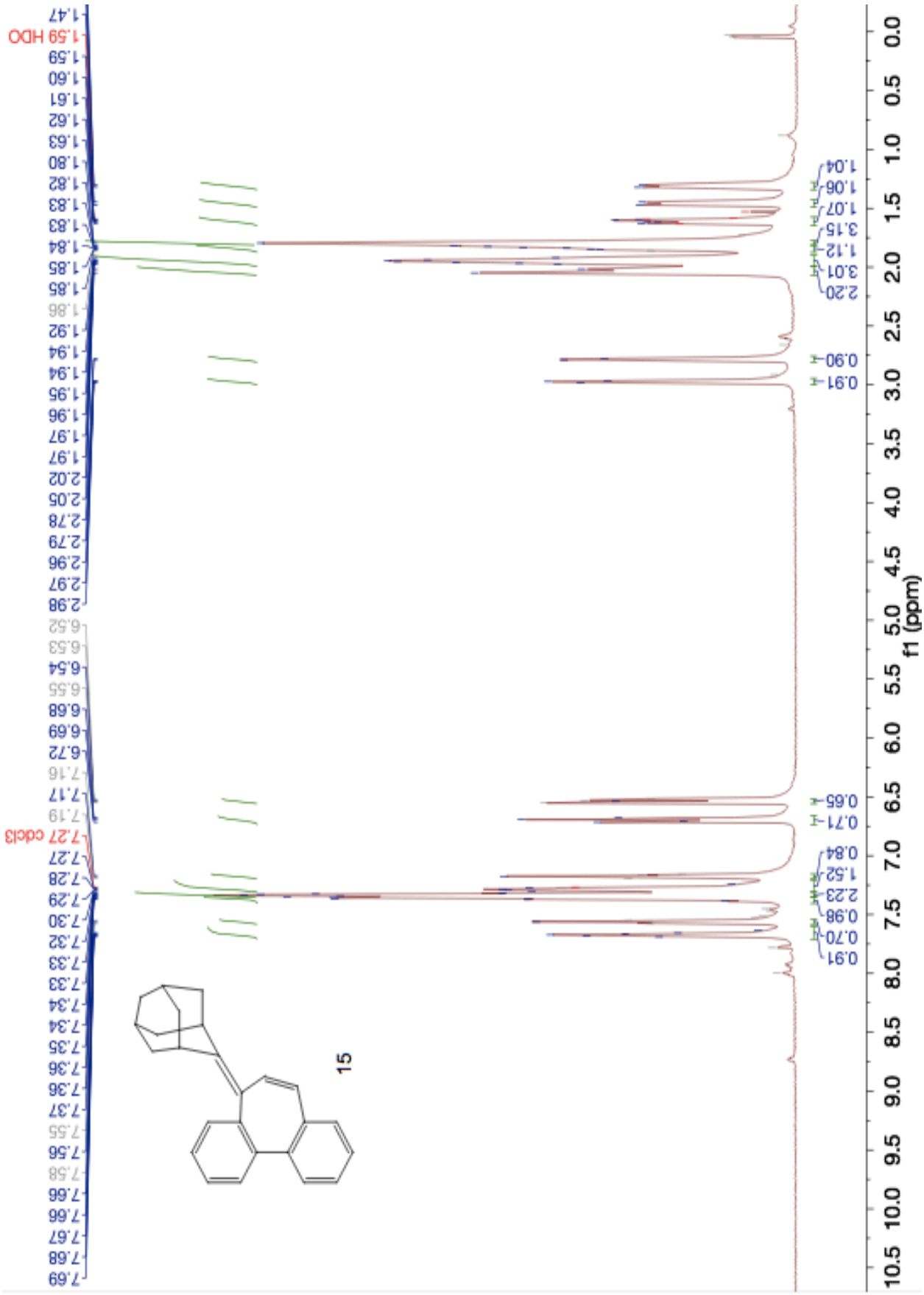
1.47
1.59 HDO
1.59
1.60
1.61
1.62
1.63
1.80
1.82
1.83
1.83
1.84
1.85
1.85
1.86
1.92
1.94
1.94
1.95
1.96
1.97
1.97
2.02
2.05
2.78
2.79
2.96
2.97
2.98
6.52
6.53
6.54
6.55
6.68
6.69
6.72
7.16
7.17
7.19
7.27 cdcl3
7.27
7.28
7.29
7.30
7.32
7.33
7.33
7.34
7.34
7.35
7.36
7.36
7.37
7.55
7.56
7.58
7.66
7.66
7.67
7.68
7.69
1.04
1.06
1.07
3.15
1.12
3.01
2.20
0.90
0.91
0.65
0.71
0.84
1.52
2.23
0.98
0.70
0.91
15
0.0
0.5
1.0
1.5
2.0
2.5
3.0
3.5
4.0
4.5
5.0
5.5
6.0
6.5
7.0
7.5
8.0
8.5
9.0
9.5
10.0
10.5
f1 (ppm)

```
File       :D:\1\data\Christine\CW01221501.D
Operator   : Christine
Acquired   : 23 Jan 2015   9:32     using AcqMethod DASLAB2MIN.M
Instrument :    GCMS1
Sample Name: adprecphotolysis
Misc Info  : hr 7
Vial Number: 1
```

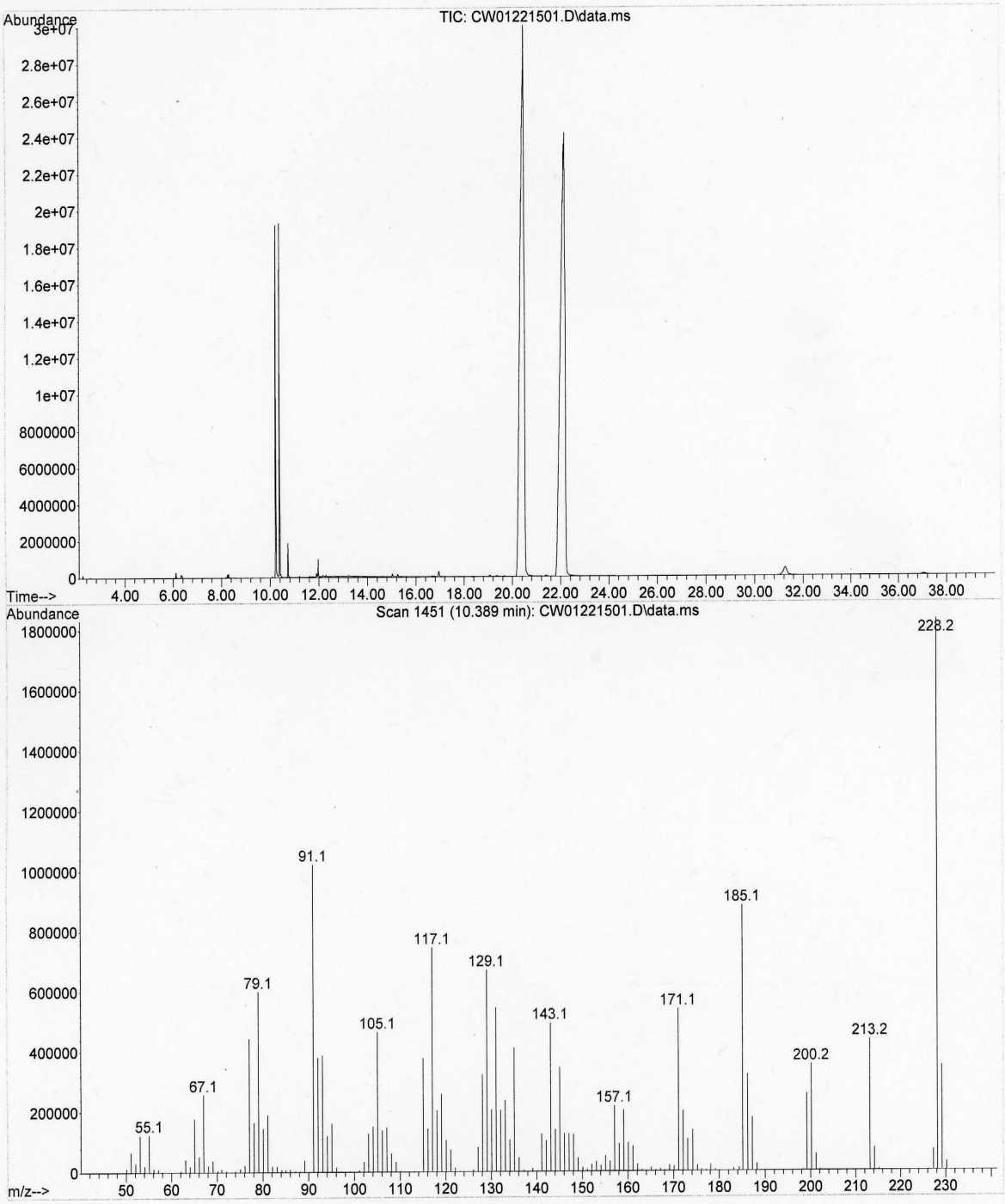

```
File       :D:\1\data\Christine\Snapshot\CW01301505.D
Operator   : Das
Acquired   : 30 Jan 2015  11:59     using AcqMethod DASLAB3MIN.M
Instrument :    GCMS1
Sample Name: Adamantylidenecarbene+Cyclohexene adduct
Misc Info  : Combined col fractions
Vial Number: 1
```

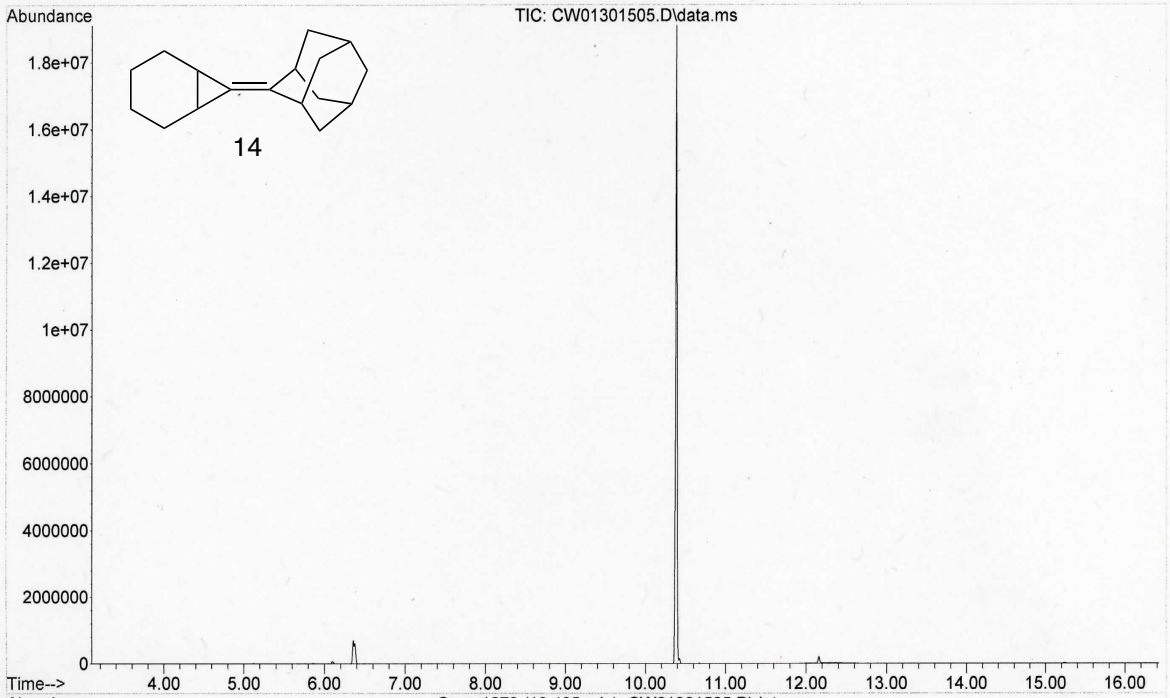

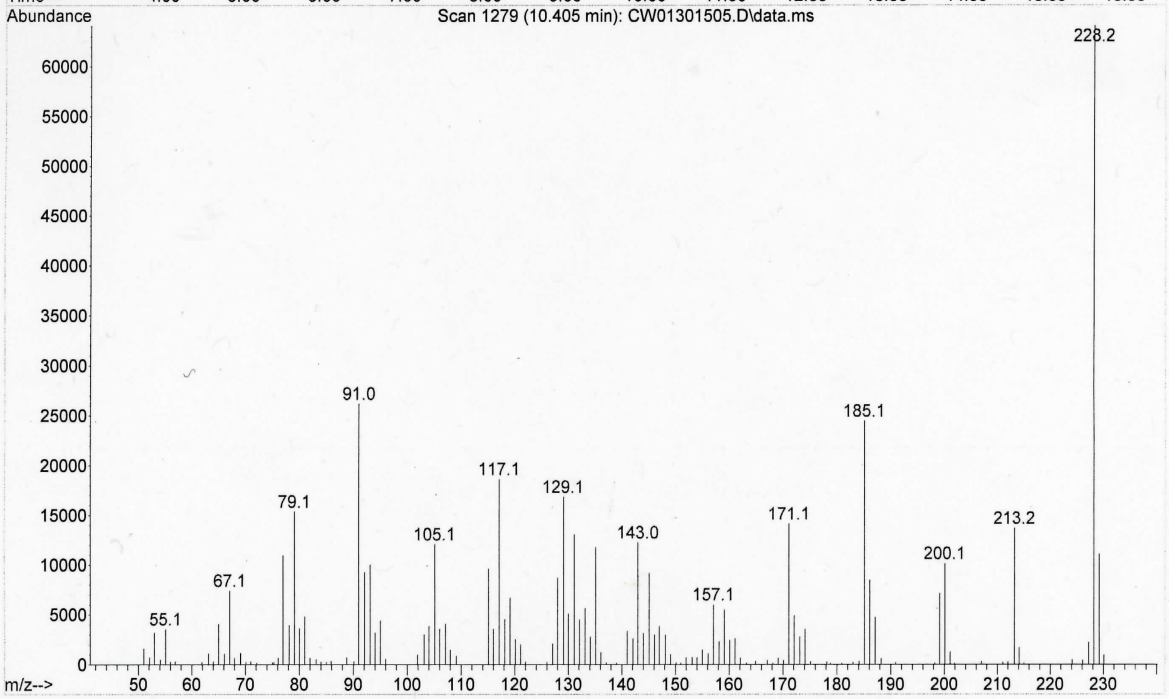

File :D:\1\data\Christine\Snapshot\CW01301503.D
Operator : Das
Acquired : 30 Jan 2015 13:33 using AcqMethod DASLAB3MIN.M
Instrument : GCMS1
Sample Name: Precursor isomer after hv
Misc Info : Combined column fractions
Vial Number: 1

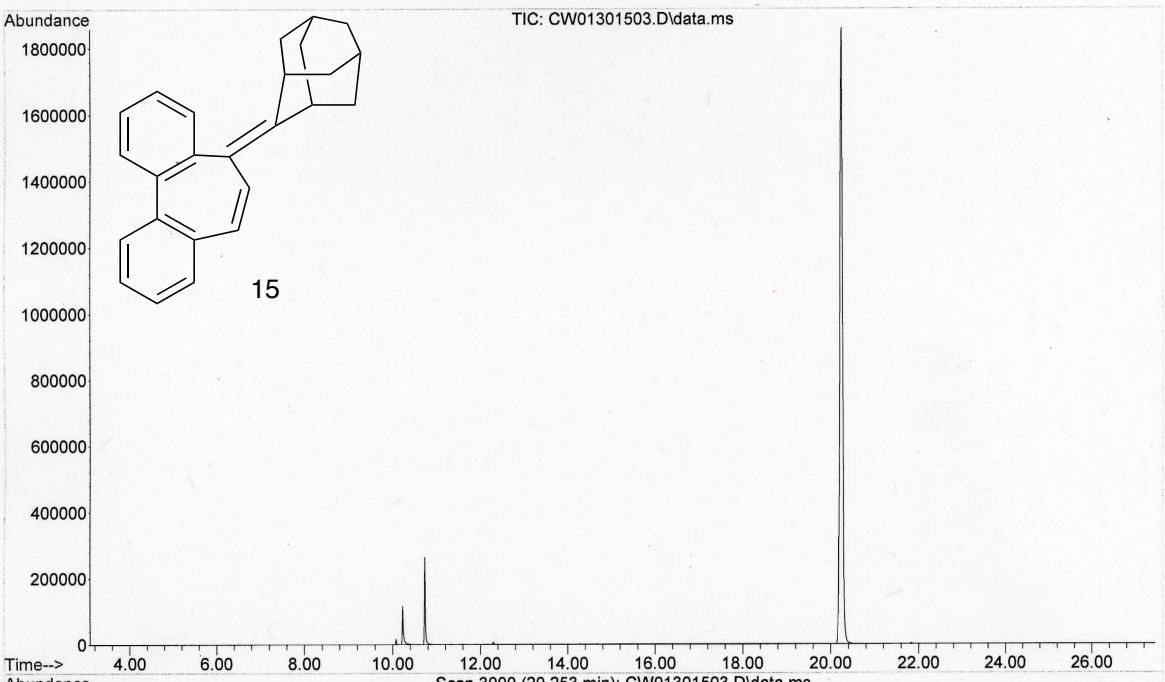

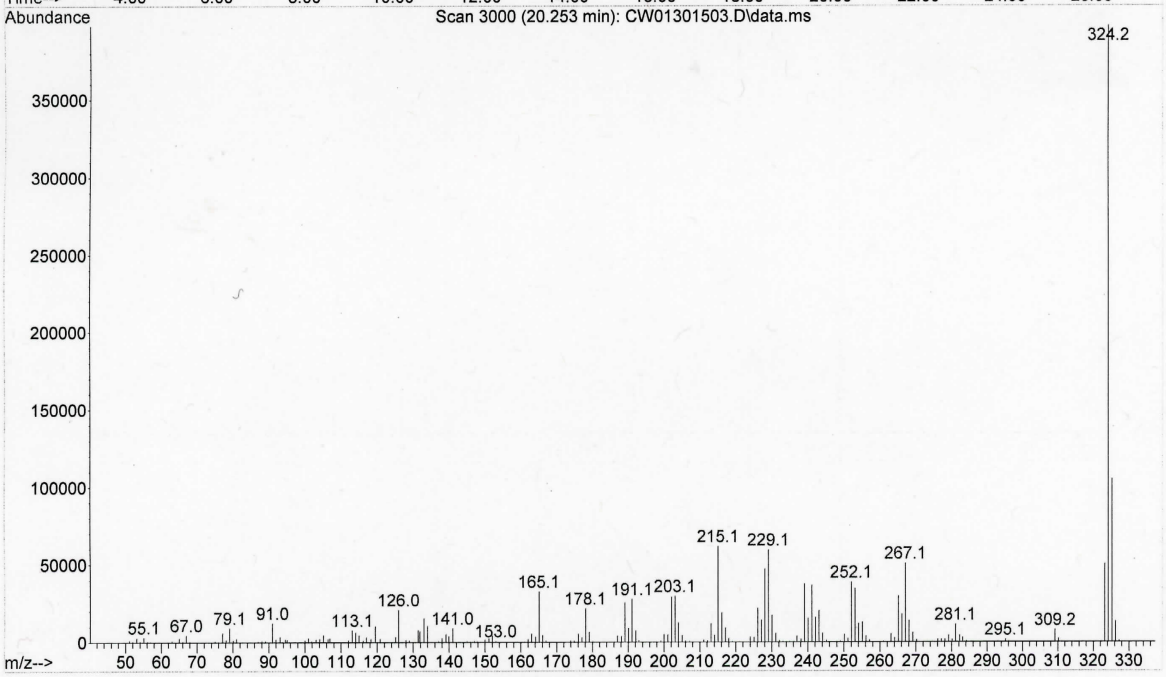

Crystal Structure Report for CWprecursor

A clear colourless plate-like specimen of $C_{25}H_{25}$, approximate dimensions 0.080 mm x 0.270 mm x 0.400 mm, was used for the X-ray crystallographic analysis. The X-ray intensity data were measured.

The total exposure time was 15.41 hours. The frames were integrated with the Bruker SAINT software package using a narrow-frame algorithm. The integration of the data using an orthorhombic unit cell yielded a total of 14935 reflections to a maximum θ angle of 26.38° (0.80 Å resolution), of which 3610 were independent (average redundancy 4.137, completeness = 99.7%, R_{int} = 2.85%, R_{sig} = 2.32%) and 3256 (90.19%) were greater than $2\sigma(F^2)$. The final cell constants of a = 6.2276(7) Å, b =11.2427(13) Å, c = 25.353(3) Å, volume = 1775.1(4) $Å^3$, are based upon the refinement of the XYZ-centroids of 5082 reflections above 20 σ(I) with 4.842° < 2θ < 52.49°. Data were corrected for absorption effects using the multi-scan method (SADABS). The ratio of minimum to maximum apparent transmission was 0.832. The calculated minimum and maximum transmission coefficients (based on crystal size) are 0.9730 and 0.9950.

The final anisotropic full-matrix least-squares refinement on F^2 with 226 variables converged at R1 = 4.24%, for the observed data and wR2 = 13.34% for all data. The goodness-of-fit was 1.024. The largest peak in the final difference electron density synthesis was 0.201 $e^-/Å^3$ and the largest hole was -0.136 $e^-/Å^3$ with an RMS deviation of 0.036 $e^-/Å^3$. On the basis of the final model, the calculated density was 1.218 g/cm^3 and F(000), 700 e^-.

Table 1. Sample and crystal data for CWprecursor.

Identification code	CWprecursor	
Chemical formula	$C_{25}H_{25}$	
Formula weight	325.45 g/mol	
Temperature	173(2) K	
Wavelength	0.71073 Å	
Crystal size	0.080 x 0.270 x 0.400 mm	
Crystal habit	clear colourless plate	
Crystal system	orthorhombic	
Space group	P 21 21 21	
Unit cell dimensions	a = 6.2276(7) Å	α = 90°
	b = 11.2427(13) Å	β = 90°
	c = 25.353(3) Å	γ = 90°
Volume	1775.1(4) $Å^3$	

Z	4
Density (calculated)	1.218 g/cm^3
Absorption coefficient	0.068 mm^{-1}
F(000)	700

Table 2. Data collection and structure refinement for CWprecursor.

Theta range for data collection	1.61 to 26.38°
Index ranges	-7<=h<=7, -14<=k<=13, -31<=l<=31
Reflections collected	14935
Independent reflections	3610 [R(int) = 0.0285]
Coverage of independent reflections	99.7%
Absorption correction	multi-scan
Max. and min. transmission	0.9950 and 0.9730
Refinement method	Full-matrix least-squares on F^2
Refinement program	SHELXL-2014/7 (Sheldrick, 2014)
Function minimized	$\Sigma\, w(F_o^2 - F_c^2)^2$
Data / restraints / parameters	3610 / 0 / 226
Goodness-of-fit on F^2	1.024
Final R indices	3256 data; I>2σ(I) R1 = 0.0424, wR2 = 0.1242
	all data R1 = 0.0480, wR2 = 0.1334
Weighting scheme	$w=1/[\sigma^2(F_o^2)+(0.1000P)^2]$ where $P=(F_o^2+2F_c^2)/3$
Absolute structure parameter	0.9(10)
Largest diff. peak and hole	0.201 and -0.136 eÅ^{-3}
R.M.S. deviation from mean	0.036 eÅ^{-3}

Table 3. Atomic coordinates and equivalent isotropic atomic displacement parameters (Å^2) for CWprecursor.

U(eq) is defined as one third of the trace of the orthogonalized U_{ij} tensor.

	x/a	y/b	z/c	U(eq)
C1	0.5396(5)	0.9397(2)	0.95562(10)	0.0488(6)
C2	0.5289(4)	0.0361(2)	0.98977(8)	0.0399(5)
C3	0.6911(4)	0.05912(17)	0.02653(8)	0.0331(4)
C4	0.8684(4)	0.98164(19)	0.02820(8)	0.0385(5)
C5	0.0388(4)	0.9946(2)	0.06856(9)	0.0446(6)
C6	0.9712(4)	0.9851(2)	0.12402(9)	0.0400(5)
C7	0.8632(3)	0.92117(18)	0.15832(8)	0.0342(5)
C8	0.8032(4)	0.7928(2)	0.14873(9)	0.0425(5)
C9	0.5613(5)	0.7896(2)	0.13972(11)	0.0561(7)

	x/a	y/b	z/c	U(eq)
C10	0.4482(4)	0.8406(3)	0.18721(13)	0.0602(7)
C11	0.4997(5)	0.7646(3)	0.23568(13)	0.0642(8)
C12	0.8582(4)	0.7162(2)	0.19718(10)	0.0487(6)
C13	0.7435(4)	0.7663(2)	0.24556(10)	0.0524(7)
C14	0.8187(5)	0.8943(3)	0.25504(9)	0.0554(7)
C15	0.7611(4)	0.9715(2)	0.20719(8)	0.0404(5)
C16	0.0261(4)	0.1049(2)	0.10554(9)	0.0430(6)
C17	0.7160(5)	0.8655(2)	0.95670(10)	0.0527(7)
C18	0.8782(4)	0.8872(2)	0.99229(9)	0.0492(6)
C19	0.6823(4)	0.16651(18)	0.06115(7)	0.0328(4)
C20	0.8498(4)	0.19106(19)	0.09685(8)	0.0379(5)
C21	0.8449(5)	0.2963(2)	0.12600(8)	0.0493(6)
C22	0.6755(5)	0.3744(2)	0.12204(9)	0.0526(7)
C23	0.5083(5)	0.3507(2)	0.08812(9)	0.0478(6)
C24	0.5131(4)	0.24819(19)	0.05761(8)	0.0377(5)
C25	0.5180(4)	0.9683(2)	0.19747(12)	0.0550(7)

Table 4. Bond lengths (Å) for CWprecursor.

C1-C17	1.380(4)	C1-C2	1.389(3)
C1-H1	0.95	C2-C3	1.399(3)
C2-H11	0.95	C3-C4	1.407(3)
C3-C19	1.494(3)	C4-C18	1.400(3)
C4-C5	1.481(3)	C5-C6	1.472(3)
C5-C16	1.556(4)	C5-H10	1.0
C6-C7	1.313(3)	C6-C16	1.466(3)
C7-C15	1.503(3)	C7-C8	1.511(3)
C8-C9	1.524(4)	C8-C12	1.539(3)
C8-H5	1.0	C9-C10	1.508(5)
C9-H24	0.99	C9-H4	0.99
C10-C25	1.523(4)	C10-C11	1.530(4)
C10-H25	1.0	C11-C13	1.539(4)
C11-H2	0.99	C11-H3	0.99
C12-C13	1.527(4)	C12-H6	0.99
C12-H23	0.99	C13-C14	1.532(4)
C13-H22	1.0	C14-C15	1.534(3)
C14-H7	0.99	C14-H21	0.99
C15-C25	1.534(4)	C15-H8	1.0
C16-C20	1.481(3)	C16-H18	1.0
C17-C18	1.376(4)	C17-H12	0.95
C18-H13	0.95	C19-C24	1.401(3)
C19-C20	1.408(3)	C20-C21	1.395(3)

C21-C22	1.376(4)	C21-H17	0.95
C22-C23	1.376(4)	C22-H16	0.95
C23-C24	1.388(3)	C23-H14	0.95
C24-H15	0.95	C25-H20	0.99
C25-H19	0.99		

Table 5. Bond angles (°) for CWprecursor.

C17-C1-C2	119.8(2)	C17-C1-H1	120.1
C2-C1-H1	120.1	C1-C2-C3	121.7(2)
C1-C2-H11	119.2	C3-C2-H11	119.2
C2-C3-C4	118.19(19)	C2-C3-C19	120.96(19)
C4-C3-C19	120.77(19)	C18-C4-C3	119.0(2)
C18-C4-C5	119.5(2)	C3-C4-C5	121.5(2)
C6-C5-C4	116.62(19)	C6-C5-C16	57.84(16)
C4-C5-C16	117.27(18)	C6-C5-H10	117.3
C4-C5-H10	117.3	C16-C5-H10	117.3
C7-C6-C16	146.4(2)	C7-C6-C5	145.0(2)
C16-C6-C5	63.98(16)	C6-C7-C15	123.8(2)
C6-C7-C8	122.9(2)	C15-C7-C8	112.83(18)
C7-C8-C9	106.93(19)	C7-C8-C12	110.57(19)
C9-C8-C12	109.0(2)	C7-C8-H5	110.1
C9-C8-H5	110.1	C12-C8-H5	110.1
C10-C9-C8	109.4(2)	C10-C9-H24	109.8
C8-C9-H24	109.8	C10-C9-H4	109.8
C8-C9-H4	109.8	H24-C9-H4	108.2
C9-C10-C25	111.2(2)	C9-C10-C11	109.3(2)
C25-C10-C11	109.2(3)	C9-C10-H25	109.0
C25-C10-H25	109.0	C11-C10-H25	109.0
C10-C11-C13	109.3(2)	C10-C11-H2	109.8
C13-C11-H2	109.8	C10-C11-H3	109.8
C13-C11-H3	109.8	H2-C11-H3	108.3
C13-C12-C8	109.29(19)	C13-C12-H6	109.8
C8-C12-H6	109.8	C13-C12-H23	109.8
C8-C12-H23	109.8	H6-C12-H23	108.3
C12-C13-C14	109.3(2)	C12-C13-C11	109.0(2)
C14-C13-C11	109.8(2)	C12-C13-H22	109.6
C14-C13-H22	109.6	C11-C13-H22	109.6
C13-C14-C15	109.63(19)	C13-C14-H7	109.7
C15-C14-H7	109.7	C13-C14-H21	109.7
C15-C14-H21	109.7	H7-C14-H21	108.2
C7-C15-C25	106.0(2)	C7-C15-C14	109.85(19)
C25-C15-C14	110.1(2)	C7-C15-H8	110.3

C25-C15-H8	110.3	C14-C15-H8	110.3
C6-C16-C20	118.42(19)	C6-C16-C5	58.18(15)
C20-C16-C5	117.99(18)	C6-C16-H18	116.5
C20-C16-H18	116.5	C5-C16-H18	116.5
C18-C17-C1	119.4(2)	C18-C17-H12	120.3
C1-C17-H12	120.3	C17-C18-C4	121.9(2)
C17-C18-H13	119.0	C4-C18-H13	119.0
C24-C19-C20	118.02(18)	C24-C19-C3	121.33(18)
C20-C19-C3	120.60(19)	C21-C20-C19	119.4(2)
C21-C20-C16	119.5(2)	C19-C20-C16	121.1(2)
C22-C21-C20	121.3(2)	C22-C21-H17	119.4
C20-C21-H17	119.4	C21-C22-C23	120.1(2)
C21-C22-H16	119.9	C23-C22-H16	119.9
C22-C23-C24	119.5(2)	C22-C23-H14	120.2
C24-C23-H14	120.2	C23-C24-C19	121.6(2)
C23-C24-H15	119.2	C19-C24-H15	119.2
C10-C25-C15	109.4(2)	C10-C25-H20	109.8
C15-C25-H20	109.8	C10-C25-H19	109.8
C15-C25-H19	109.8	H20-C25-H19	108.3

Table 6. Torsion angles (°) for CWprecursor.

C17-C1-C2-C3	-1.5(3)	C1-C2-C3-C4	0.1(3)
C1-C2-C3-C19	177.0(2)	C2-C3-C4-C18	1.7(3)
C19-C3-C4-C18	-175.12(18)	C2-C3-C4-C5	-175.39(19)
C19-C3-C4-C5	7.8(3)	C18-C4-C5-C6	-117.4(2)
C3-C4-C5-C6	59.7(3)	C18-C4-C5-C16	176.92(18)
C3-C4-C5-C16	-6.0(3)	C4-C5-C6-C7	49.9(4)
C16-C5-C6-C7	156.8(4)	C4-C5-C6-C16	-106.9(2)
C16-C6-C7-C15	-12.9(5)	C5-C6-C7-C15	-153.1(3)
C16-C6-C7-C8	158.3(3)	C5-C6-C7-C8	18.2(5)
C6-C7-C8-C9	-109.0(2)	C15-C7-C8-C9	63.1(2)
C6-C7-C8-C12	132.4(2)	C15-C7-C8-C12	-55.5(2)
C7-C8-C9-C10	-58.4(3)	C12-C8-C9-C10	61.2(3)
C8-C9-C10-C25	59.2(3)	C8-C9-C10-C11	-61.5(3)
C9-C10-C11-C13	60.7(3)	C25-C10-C11-C13	-61.1(3)
C7-C8-C12-C13	56.9(3)	C9-C8-C12-C13	-60.4(3)
C8-C12-C13-C14	-60.3(3)	C8-C12-C13-C11	59.7(3)
C10-C11-C13-C12	-59.8(3)	C10-C11-C13-C14	59.8(3)
C12-C13-C14-C15	61.3(3)	C11-C13-C14-C15	-58.3(3)
C6-C7-C15-C25	108.9(2)	C8-C7-C15-C25	-63.2(2)
C6-C7-C15-C14	-132.1(2)	C8-C7-C15-C14	55.8(3)
C13-C14-C15-C7	-58.1(3)	C13-C14-C15-C25	58.3(3)

C7-C6-C16-C20	-48.9(5)	C5-C6-C16-C20	107.0(2)
C7-C6-C16-C5	-155.9(4)	C4-C5-C16-C6	105.8(2)
C6-C5-C16-C20	-107.7(2)	C4-C5-C16-C20	-2.0(3)
C2-C1-C17-C18	0.9(4)	C1-C17-C18-C4	1.0(3)
C3-C4-C18-C17	-2.3(3)	C5-C4-C18-C17	174.8(2)
C2-C3-C19-C24	-0.7(3)	C4-C3-C19-C24	176.09(18)
C2-C3-C19-C20	-177.93(19)	C4-C3-C19-C20	-1.2(3)
C24-C19-C20-C21	-1.9(3)	C3-C19-C20-C21	175.46(18)
C24-C19-C20-C16	175.59(18)	C3-C19-C20-C16	-7.1(3)
C6-C16-C20-C21	118.9(2)	C5-C16-C20-C21	-174.10(19)
C6-C16-C20-C19	-58.5(3)	C5-C16-C20-C19	8.4(3)
C19-C20-C21-C22	2.6(3)	C16-C20-C21-C22	-175.0(2)
C20-C21-C22-C23	-1.3(4)	C21-C22-C23-C24	-0.6(4)
C22-C23-C24-C19	1.3(3)	C20-C19-C24-C23	0.0(3)
C3-C19-C24-C23	-177.30(19)	C9-C10-C25-C15	-59.7(3)
C11-C10-C25-C15	61.0(3)	C7-C15-C25-C10	59.0(3)
C14-C15-C25-C10	-59.8(3)		

Table 7. Anisotropic atomic displacement parameters (Å^2) for CWprecursor.

The anisotropic atomic displacement factor exponent takes the form: $-2\pi^2[h^2 a^{*2} U_{11} + ... + 2 h k a^* b^* U_{12}]$

	U_{11}	U_{22}	U_{33}	U_{23}	U_{13}	U_{12}
C1	0.0575(15)	0.0393(12)	0.0496(13)	-0.0069(10)	0.0007(12)	-0.0091(11)
C2	0.0425(11)	0.0360(11)	0.0411(11)	0.0006(9)	0.0025(9)	-0.0026(10)
C3	0.0382(11)	0.0277(10)	0.0335(9)	0.0062(7)	0.0056(8)	-0.0012(9)
C4	0.0406(11)	0.0374(11)	0.0375(10)	0.0112(8)	0.0112(9)	0.0046(10)
C5	0.0357(10)	0.0487(13)	0.0494(12)	0.0173(10)	0.0101(10)	0.0107(10)
C6	0.0333(10)	0.0434(12)	0.0432(11)	0.0121(9)	-0.0020(9)	0.0055(9)
C7	0.0322(10)	0.0355(10)	0.0347(9)	0.0074(8)	-0.0025(8)	0.0033(9)
C8	0.0518(13)	0.0327(11)	0.0431(11)	0.0012(9)	0.0022(10)	0.0045(10)
C9	0.0627(16)	0.0407(13)	0.0648(16)	0.0055(12)	-0.0289(14)	-0.0107(12)
C10	0.0286(11)	0.0580(16)	0.094(2)	0.0161(14)	-0.0056(13)	-0.0036(11)
C11	0.0515(16)	0.0647(18)	0.0764(19)	0.0171(15)	0.0157(14)	-0.0101(14)
C12	0.0429(12)	0.0386(12)	0.0645(14)	0.0170(11)	-0.0064(11)	-0.0003(10)
C13	0.0575(16)	0.0528(15)	0.0468(12)	0.0200(11)	-0.0062(11)	-0.0131(13)
C14	0.0716(17)	0.0606(15)	0.0339(10)	0.0073(10)	-0.0056(11)	-0.0142(14)
C15	0.0461(12)	0.0362(11)	0.0389(11)	-0.0006(9)	-0.0010(9)	-0.0032(10)
C16	0.0329(11)	0.0507(14)	0.0454(12)	0.0162(10)	-0.0049(9)	-0.0084(10)
C17	0.0737(19)	0.0354(12)	0.0491(12)	-0.0036(10)	0.0170(13)	-0.0064(12)
C18	0.0598(15)	0.0354(11)	0.0524(13)	0.0106(10)	0.0233(12)	0.0125(11)
C19	0.0381(10)	0.0308(10)	0.0295(9)	0.0058(7)	0.0022(8)	-0.0029(9)
C20	0.0421(12)	0.0368(11)	0.0346(10)	0.0113(8)	-0.0013(9)	-0.0078(9)

	U_{11}	U_{22}	U_{33}	U_{23}	U_{13}	U_{12}
C21	0.0682(17)	0.0436(12)	0.0361(11)	0.0044(9)	-0.0088(11)	-0.0149(12)
C22	0.085(2)	0.0346(11)	0.0386(11)	-0.0028(9)	-0.0011(12)	-0.0040(13)
C23	0.0658(17)	0.0365(11)	0.0410(11)	0.0024(9)	0.0037(11)	0.0081(11)
C24	0.0447(12)	0.0361(11)	0.0322(10)	0.0034(8)	-0.0013(8)	0.0030(10)
C25	0.0437(13)	0.0486(14)	0.0728(17)	0.0061(13)	0.0123(13)	0.0104(11)

Table 8. Hydrogen atomic coordinates and isotropic atomic displacement parameters (Å^2) for CWprecursor.

	x/a	y/b	z/c	U(eq)
H1	0.4257	0.9249	-0.0684	0.059
H11	0.4083	1.0877	-0.0119	0.048
H10	1.1850	0.9643	0.0594	0.054
H5	0.8800	0.7619	0.1169	0.051
H24	0.5244	0.8365	0.1079	0.067
H4	0.5140	0.7065	0.1339	0.067
H25	0.2897	0.8390	0.1809	0.072
H2	0.4509	0.6819	0.2298	0.077
H3	0.4234	0.7965	0.2669	0.077
H6	0.8122	0.6330	0.1911	0.058
H23	1.0153	0.7165	0.2031	0.058
H22	0.7780	0.7165	0.2771	0.063
H7	0.9760	0.8955	0.2607	0.066
H21	0.7486	0.9266	0.2870	0.066
H8	0.8100	1.0553	0.2129	0.048
H18	1.1658	1.1383	0.1181	0.052
H12	0.7254	0.8001	-0.0669	0.063
H13	1.0004	0.8366	-0.0075	0.059
H17	0.9608	1.3144	0.1490	0.059
H16	0.6739	1.4448	0.1428	0.063
H14	0.3906	1.4041	0.0856	0.057
H15	0.3987	1.2331	0.0337	0.045
H20	0.4414	1.0001	0.2286	0.066
H19	0.4817	1.0186	0.1667	0.066

2-Adamantylidenecarbene, singlet (DFT)

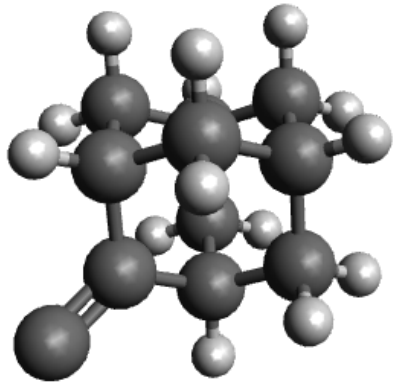

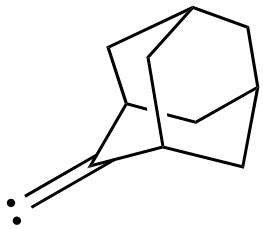

SCF Done: E(RB3LYP) = -427.485519412 A.U. after 13 cycles

Center Number	Atomic Number	Atomic Type	Coordinates (Angstroms) X	Y	Z
1	6	0	0.175133	1.245586	-1.244976
2	1	0	-0.464077	1.257907	-2.164313
3	1	0	0.815714	2.163967	-1.256266
4	6	0	1.056728	0.000363	-1.245320
5	1	0	1.706086	0.000621	-2.160595
6	6	0	-0.708279	1.246679	-0.001056
7	1	0	-1.356223	2.162959	-0.001807
8	6	0	0.175161	-1.244874	-1.245641
9	1	0	0.815770	-2.163235	-1.257313
10	1	0	-0.464055	-1.256939	-2.164979
11	6	0	-0.708300	-1.246674	-0.001747
12	1	0	-1.356219	-2.162966	-0.003021
13	6	0	0.171293	-1.245593	1.244868
14	1	0	-0.470730	-1.258258	2.162234
15	1	0	0.811890	-2.163949	1.257975
16	6	0	1.934293	-0.000039	0.002723
17	1	0	2.592473	0.905887	0.003994
18	1	0	2.592342	-0.906075	0.003490
19	6	0	0.171358	1.244933	1.245534
20	1	0	0.812014	2.163242	1.259049
21	1	0	-0.470653	1.257179	2.162914
22	6	0	1.052832	-0.000347	1.248025
23	1	0	1.699329	-0.000610	2.165320
24	6	0	-1.587815	0.000014	-0.002742
25	6	0	-2.943014	-0.000003	-0.000781

2-Adamantylidenecarbene, triplet (DFT)

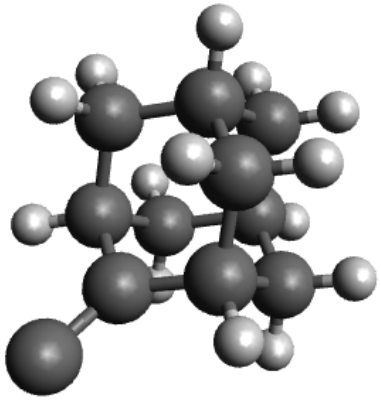

SCF Done: E(UB3LYP) = -427.414116827 A.U. after 20 cycles

Center Number	Atomic Number	Atomic Type	Coordinates (Angstroms) X	Y	Z
1	6	0	0.175133	1.245586	-1.244976
2	1	0	-0.464077	1.257907	-2.164313
3	1	0	0.815714	2.163967	-1.256266
4	6	0	1.056728	0.000363	-1.245320
5	1	0	1.706086	0.000621	-2.160595
6	6	0	-0.708279	1.246679	-0.001056
7	1	0	-1.356223	2.162959	-0.001807
8	6	0	0.175161	-1.244874	-1.245641
9	1	0	0.815770	-2.163235	-1.257313
10	1	0	-0.464055	-1.256939	-2.164979
11	6	0	-0.708300	-1.246674	-0.001747
12	1	0	-1.356219	-2.162966	-0.003021
13	6	0	0.171293	-1.245593	1.244868
14	1	0	-0.470730	-1.258258	2.162234
15	1	0	0.811890	-2.163949	1.257975
16	6	0	1.934293	-0.000039	0.002723
17	1	0	2.592473	0.905887	0.003994
18	1	0	2.592342	-0.906075	0.003490
19	6	0	0.171358	1.244933	1.245534
20	1	0	0.812014	2.163242	1.259049
21	1	0	-0.470653	1.257179	2.162914
22	6	0	1.052832	-0.000347	1.248025
23	1	0	1.699329	-0.000610	2.165320
24	6	0	-1.587815	0.000014	-0.002742
25	6	0	-2.943014	-0.000003	-0.000781

Transition State (DFT)

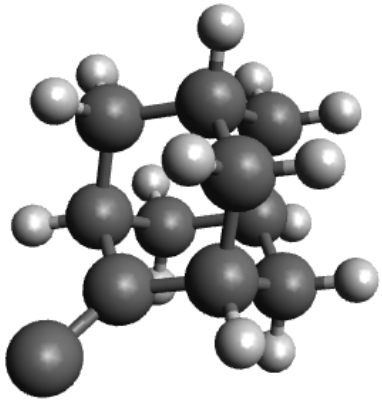

SCF Done: E(RB3LYP) = -427.443183609 A.U. after 15 cycles

Center Number	Atomic Number	Atomic Type	Coordinates (Angstroms) X	Y	Z
1	6	0	-0.746797	1.110296	1.283435
2	1	0	-0.188219	1.464566	2.158419
3	1	0	-1.761675	1.527335	1.361938
4	6	0	-0.848358	-0.436505	1.273090
5	1	0	-1.390730	-0.733794	2.181058
6	6	0	-0.093254	1.636101	-0.013237
7	1	0	-0.133857	2.730552	0.000194
8	6	0	0.506926	-1.210078	1.271391
9	1	0	0.272913	-2.282739	1.339947
10	1	0	1.110341	-0.952606	2.150432
11	6	0	1.351090	-0.964965	-0.010310
12	1	0	2.232270	-1.615245	-0.027912
13	6	0	0.474497	-1.211219	-1.269557
14	1	0	1.054123	-0.953818	-2.164483
15	1	0	0.245278	-2.285637	-1.325666
16	6	0	-1.649371	-0.864593	0.018280
17	1	0	-2.645486	-0.399699	0.025458
18	1	0	-1.804533	-1.952847	0.025302
19	6	0	-0.768406	1.092590	-1.286540
20	1	0	-1.783428	1.511575	-1.351680
21	1	0	-0.225271	1.432157	-2.176941
22	6	0	-0.875003	-0.447785	-1.253954
23	1	0	-1.434417	-0.753276	-2.148763
24	6	0	1.317734	1.117149	0.015203
25	6	0	2.406390	0.722921	-0.035684

Homoadamantyne (DFT)

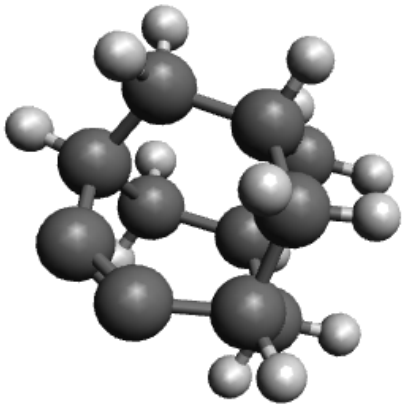

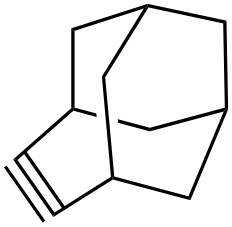

SCF Done: E(RB3LYP) = -427.376427709 A.U. after 12 cycles

Center Number	Atomic Number	Atomic Type	Coordinates (Angstroms) X	Y	Z
1	6	0	1.266034	1.388390	0.083823
2	1	0	2.130812	1.413806	-0.545790
3	1	0	1.304865	2.190245	0.791227
4	6	0	1.256517	0.000000	0.910538
5	1	0	2.140532	0.000000	1.513379
6	6	0	0.000000	1.584111	-0.794099
7	1	0	0.000000	2.533748	-1.287140
8	6	0	1.266034	-1.388390	0.083823
9	1	0	1.304865	-2.190245	0.791227
10	1	0	2.130812	-1.413806	-0.545790
11	6	0	0.000000	-1.584111	-0.794099
12	1	0	0.000000	-2.533748	-1.287140
13	6	0	-1.266034	-1.388390	0.083823
14	1	0	-2.130812	-1.413806	-0.545790
15	1	0	-1.304865	-2.190245	0.791227
16	6	0	0.000000	0.000000	1.794332
17	1	0	0.000000	0.873875	2.411780
18	1	0	0.000000	-0.873875	2.411780
19	6	0	-1.266034	1.388390	0.083823
20	1	0	-1.304865	2.190245	0.791227
21	1	0	-2.130812	1.413806	-0.545790
22	6	0	-1.256517	0.000000	0.910538
23	1	0	-2.140532	0.000000	1.513379
24	6	0	0.000000	0.512231	-1.702732
25	6	0	0.000000	-0.512231	-1.702732

2-Adamantylidenecarbene, singlet (CCSD)

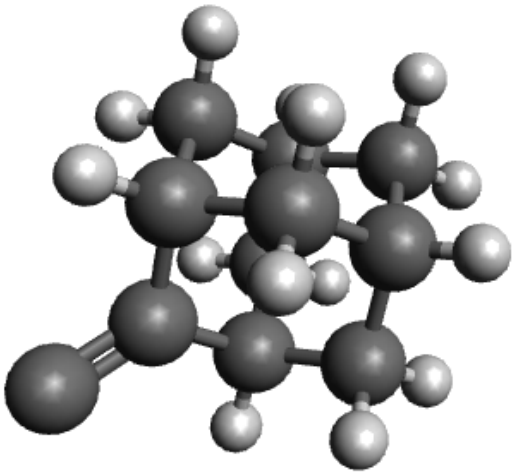

SCF Done: E(RHF) = -424.735277225 A.U. after 14 cycles

Center Number	Atomic Number	Atomic Type	Coordinates (Angstroms) X	Y	Z
1	6	0	0.163279	1.262027	-1.266893
2	1	0	-0.467044	1.287273	-2.164727
3	1	0	0.788676	2.166123	-1.281536
4	6	0	1.053028	-0.000010	-1.264044
5	1	0	1.686711	-0.000017	-2.160932
6	6	0	-0.722842	1.283241	-0.000075
7	1	0	-1.370053	2.166322	-0.000120
8	6	0	0.163253	-1.262028	-1.266891
9	1	0	0.788633	-2.166137	-1.281535
10	1	0	-0.467071	-1.287262	-2.164725
11	6	0	-0.722867	-1.283224	-0.000073
12	1	0	-1.370093	-2.166293	-0.000116
13	6	0	0.163041	-1.262015	1.266898
14	1	0	-0.467433	-1.287234	2.164627
15	1	0	0.788417	-2.166123	1.281664
16	6	0	1.940744	-0.000018	0.000142
17	1	0	2.596408	0.882421	0.000194
18	1	0	2.596390	-0.882471	0.000195
19	6	0	0.163066	1.262017	1.266896
20	1	0	0.788459	2.166113	1.281660
21	1	0	-0.467407	1.287250	2.164625
22	6	0	1.052824	-0.000008	1.264188
23	1	0	1.686360	-0.000013	2.161178
24	6	0	-1.568306	0.000019	-0.000182
25	6	0	-2.870377	0.000006	-0.000041

2-Adamantylidenecarbene, triplet (CCSD)

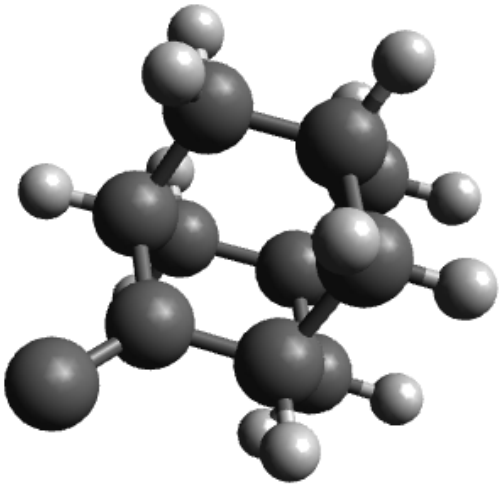

SCF Done: E(UHF) = -424.689072917 A.U. after 28 cycles

Center Number	Atomic Number	Atomic Type	Coordinates (Angstroms) X	Y	Z
1	6	0	-0.110018	1.257215	1.263848
2	1	0	0.559082	1.287176	2.133169
3	1	0	-0.724206	2.168029	1.295820
4	6	0	-1.000317	-0.000002	1.306910
5	1	0	-1.585006	-0.000003	2.237000
6	6	0	0.730401	1.260090	-0.045425
7	1	0	1.383253	2.138192	-0.079814
8	6	0	-0.110018	-1.257218	1.263844
9	1	0	-0.724206	-2.168033	1.295813
10	1	0	0.559082	-1.287183	2.133165
11	6	0	0.730401	-1.260090	-0.045429
12	1	0	1.383253	-2.138192	-0.079820
13	6	0	-0.241117	-1.254277	-1.266497
14	1	0	0.332142	-1.281184	-2.202129
15	1	0	-0.849060	-2.169038	-1.233315
16	6	0	-1.954445	0.000000	0.093378
17	1	0	-2.608553	0.882662	0.126874
18	1	0	-2.608553	-0.882665	0.126871
19	6	0	-0.241117	1.254281	-1.266493
20	1	0	-0.849061	2.169042	-1.233308
21	1	0	0.332142	1.281191	-2.202125
22	6	0	-1.133178	0.000002	-1.213379
23	1	0	-1.811901	0.000003	-2.077492
24	6	0	1.561592	0.000000	-0.112166
25	6	0	2.969748	0.000000	-0.018709

Transition State (CCSD)

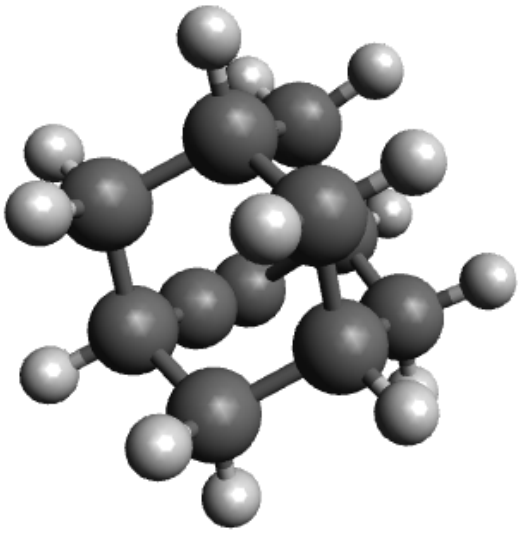

E(RHF) = -424.695813635 A.U. after 15 cycles

Center Number	Atomic Number	Atomic Type	Coordinates (Angstroms) X	Y	Z
1	6	0	-0.841635	1.054371	1.273699
2	1	0	-0.327285	1.430416	2.166180
3	1	0	-1.873983	1.428946	1.304228
4	6	0	-0.856009	-0.489814	1.261085
5	1	0	-1.386221	-0.837577	2.157801
6	6	0	-0.146743	1.599920	0.000173
7	1	0	-0.157155	2.697921	0.000304
8	6	0	0.567930	-1.096832	1.280651
9	1	0	0.472061	-2.188676	1.386067
10	1	0	1.134902	-0.743713	2.149727
11	6	0	1.373349	-0.829998	-0.001009
12	1	0	2.261836	-1.458771	-0.001908
13	6	0	0.566232	-1.096217	-1.281809
14	1	0	1.132050	-0.742496	-2.151392
15	1	0	0.470506	-2.188025	-1.387725
16	6	0	-1.599457	-0.981598	0.000847
17	1	0	-2.633201	-0.607886	0.001556
18	1	0	-1.658426	-2.079202	0.000710
19	6	0	-0.843448	1.054734	-1.272498
20	1	0	-1.875834	1.429319	-1.301420
21	1	0	-0.330391	1.431015	-2.165626
22	6	0	-0.857739	-0.489439	-1.260240
23	1	0	-1.389118	-0.837071	-2.156320
24	6	0	1.252218	1.151383	-0.000772
25	6	0	2.412011	0.667791	-0.000491

Homoadamantyne (CCSD)

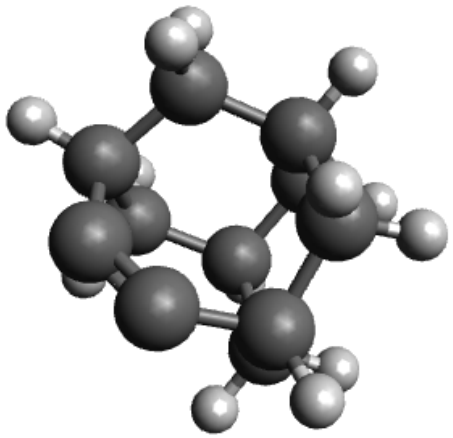

SCF Done: E(RHF) = -424.716250146 A.U. after 11 cycles

Center Number	Atomic Number	Atomic Type	Coordinates (Angstroms) X	Y	Z
1	6	0	1.279857	1.343455	0.096913
2	1	0	2.157620	1.381409	-0.559037
3	1	0	1.400589	2.149531	0.836552
4	6	0	1.245522	0.000000	0.891894
5	1	0	2.146256	0.000000	1.521676
6	6	0	0.000000	1.634644	-0.740307
7	1	0	0.000000	2.675171	-1.083664
8	6	0	1.279857	-1.343455	0.096913
9	1	0	1.400589	-2.149531	0.836552
10	1	0	2.157620	-1.381409	-0.559037
11	6	0	0.000000	-1.634644	-0.740307
12	1	0	0.000000	-2.675171	-1.083664
13	6	0	-1.279857	-1.343455	0.096913
14	1	0	-2.157620	-1.381409	-0.559037
15	1	0	-1.400589	-2.149531	0.836552
16	6	0	0.000000	0.000000	1.794862
17	1	0	0.000000	0.882866	2.449688
18	1	0	0.000000	-0.882866	2.449688
19	6	0	-1.279857	1.343455	0.096913
20	1	0	-1.400589	2.149531	0.836552
21	1	0	-2.157620	1.381409	-0.559037
22	6	0	-1.245522	0.000000	0.891894
23	1	0	-2.146256	0.000000	1.521676
24	6	0	0.000000	0.609257	-1.816632
25	6	0	0.000000	-0.609257	-1.816632